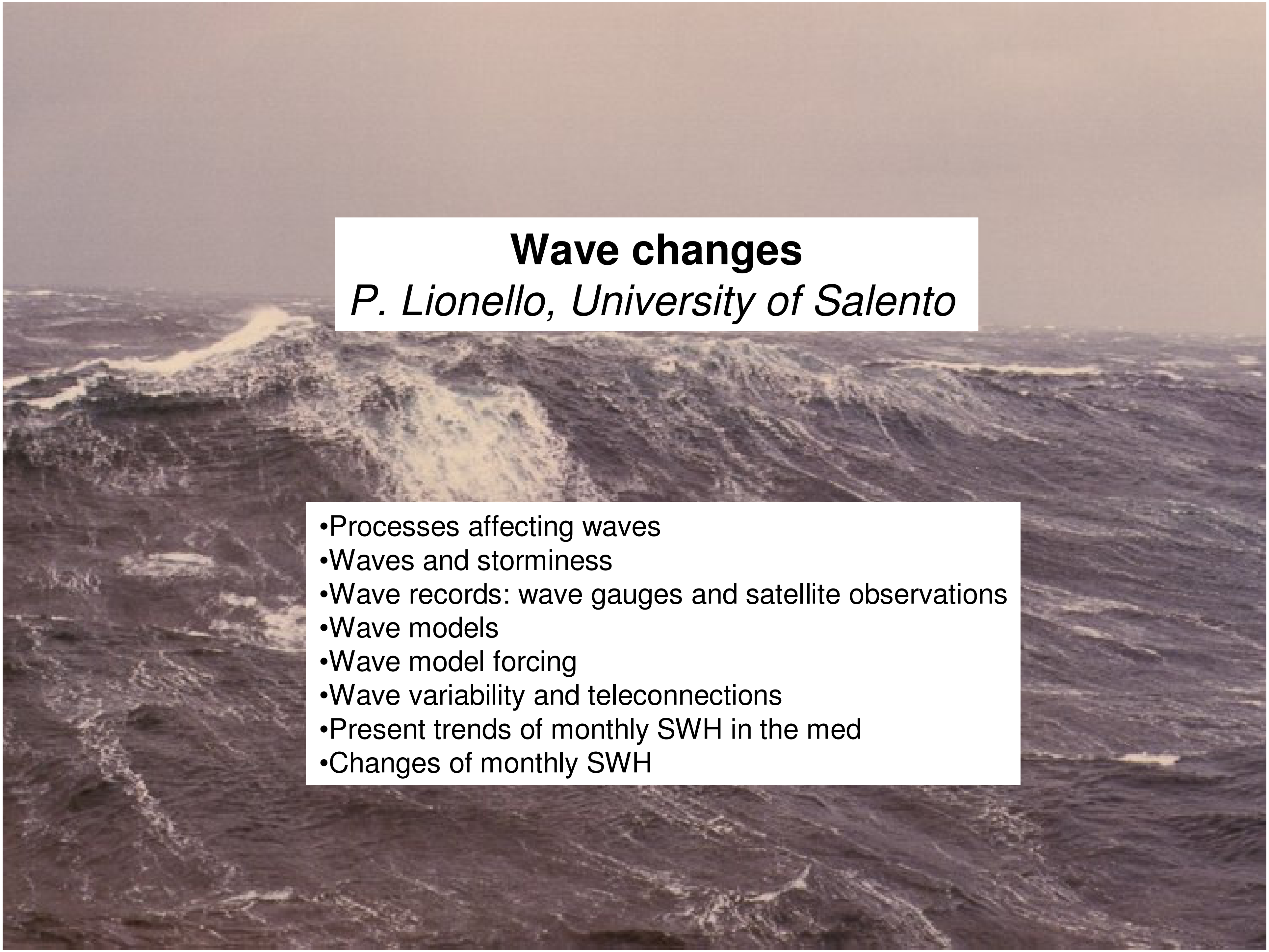

Wave changes

P. Lionello, University of Salento

- Processes affecting waves
- Waves and storminess
- Wave records: wave gauges and satellite observations
- Wave models
- Wave model forcing
- Wave variability and teleconnections
- Present trends of monthly SWH in the med
- Changes of monthly SWH

Specific References

Galati M.B., Lionello P., C..Pino (2008) **Evaluation of extreme wind wave values in the Mediterranean Sea**, in press in the proceedings of the 9th Littotal International Conference 25-28 November 2008 Venice Italy

Lionello P. and M.B.Galati (2008), **Links of the significant wave height distribution in the Mediterranean sea with the North Hemisphere teleconnection patterns** , *Adv. Geosci.* 17, 13-18

Lionello P., S.Cogo, M.B.Galati and A.Sanna, (2007), **The Mediterranean surface wave climate inferred from future scenario simulations** . *Global and Planetary Change* doi:10.1016/j.gloplacha.2008.03.004

Lionello P. and A.Sanna (2005) **Mediterranean wave climate variability and its links with NAO and Indian Monsoon** *Clim.Dyn*. , 25, 611-623

Lionello P., Bhend J., Buzzi A., Della-Marta P.M., Krichak S., Jansà A., Maheras P., Sanna A., Trigo I.F., Trigo R. (2006). **Cyclones in the Mediterranean region: climatology and effects on the environment.** In P.Lionello, P.Malanotte-Rizzoli, R.Boscolo (eds) Mediterranean Climate Variability. Amsterdam: Elsevier (NETHERLANDS), 324-272

Lionello P. (2005) **Extreme surges in the Gulf of Venice. Present and Future Climate** in Fletcher C. and T.Spencer Eds., *Venice and its lagoon, State of Knowledge* Cambridge University Press, Cambridge UK, 59-65

Lionello P., R.Mufato and A.Tomasin (2005) **Sensitivity of free and forced oscillations of the Adriatic Sea to sea level rise** *Clim. Research*., 29: 23-39

Lionello P., E.Elvini, A.Nizzero (2003) **Ocean waves and storm surges in the Adriatic Sea: intercomparison between the present and doubled CO2 climate scenarios** Clim. Research., 23: 217-231

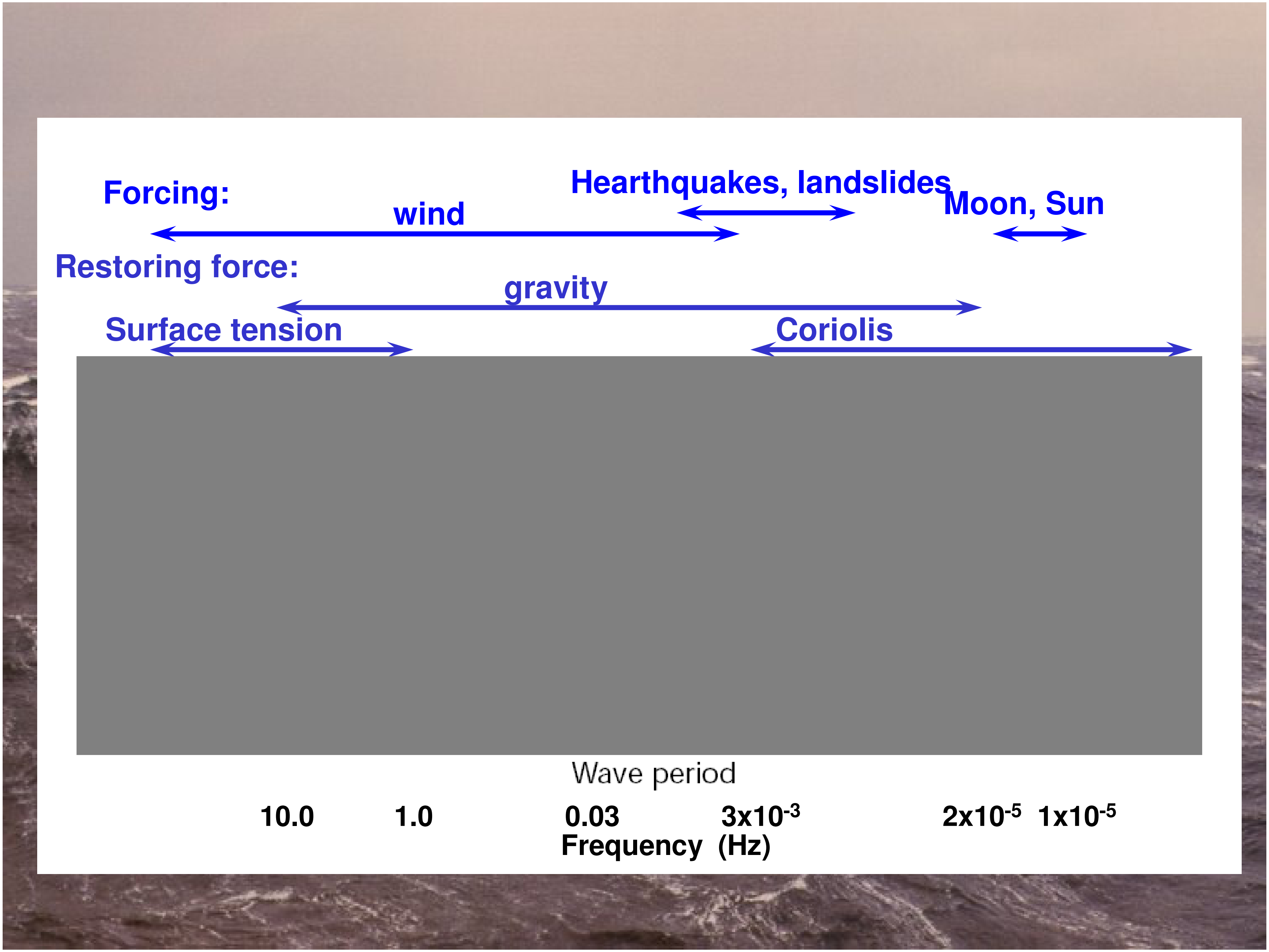
Forcing:
wind
Hearthquakes, landslides
Moon, Sun
Restoring force:
gravity
Surface tension
Coriolis
Wave period
10.0
1.0
0.03
3x10-3
2x10-5
1x10-5
Frequency (Hz)

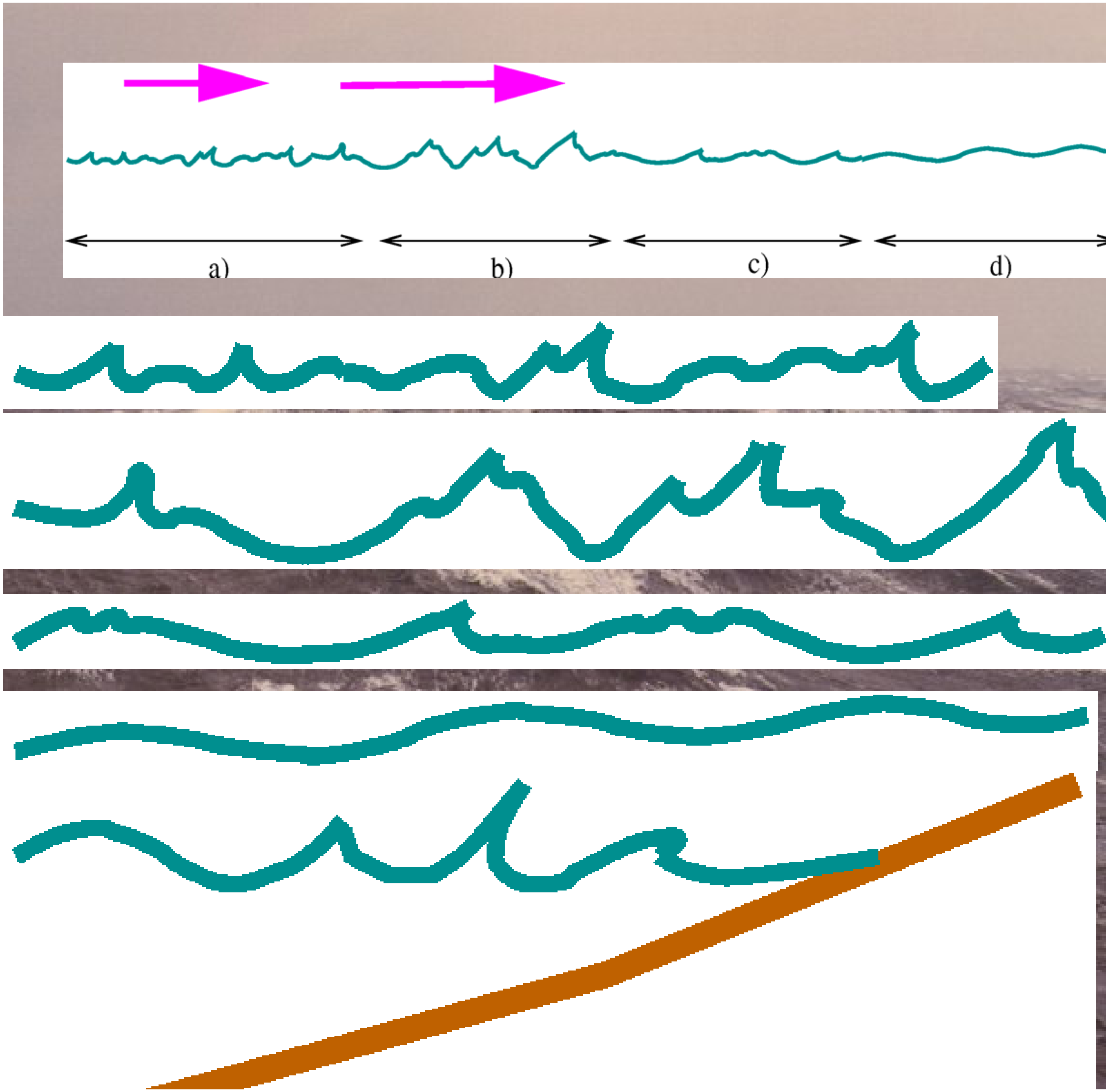

Cartoon showing the waves at different stages of their development. Parts a) and b) show the beginning and the end of wave generation during a storm; c) e d) the beginning and end of wave dispersion as they travel across the ocean, e) dissipation due to wave breaking at the coast

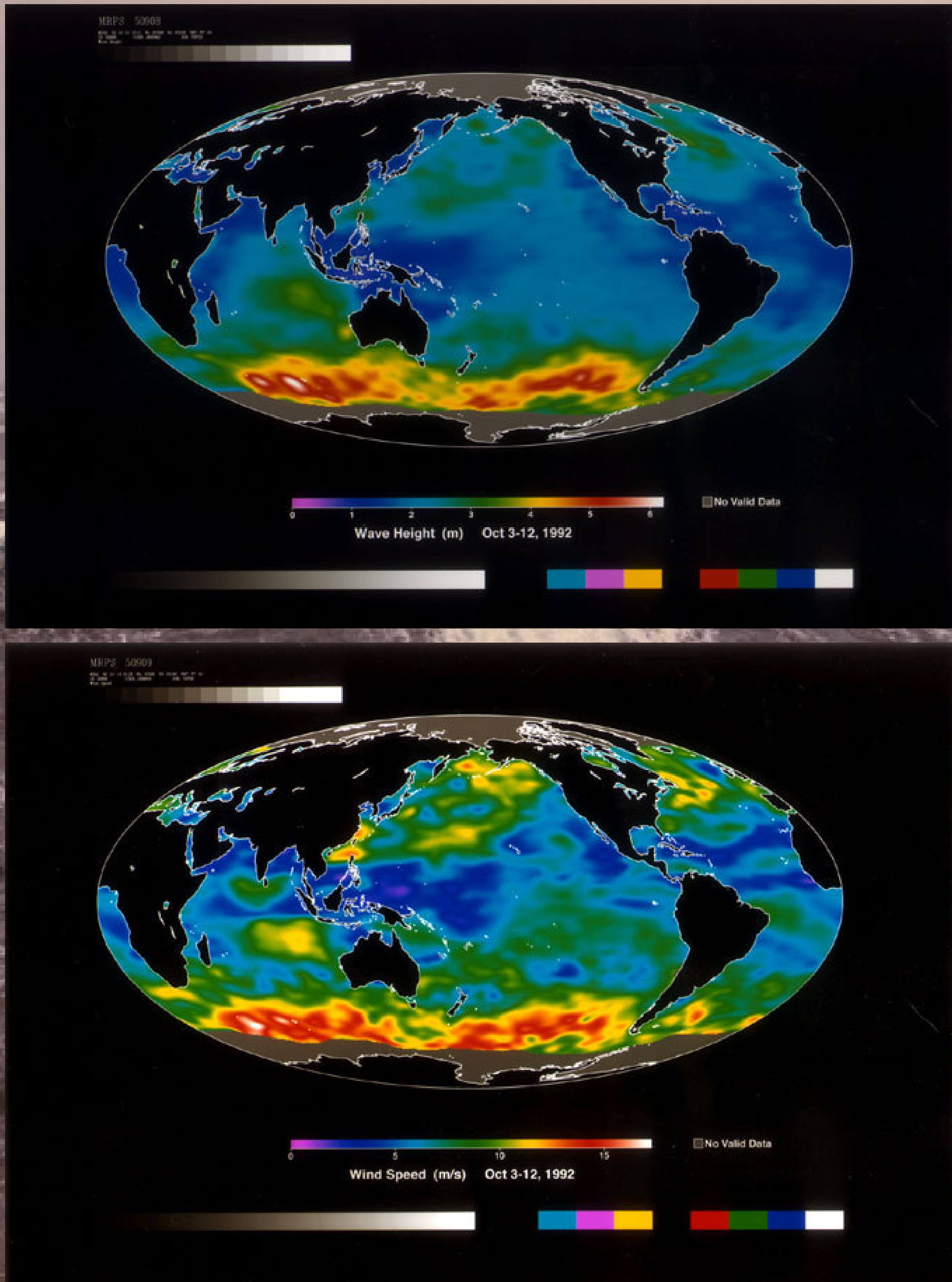

Wind speed (upper panel) and significant wave height (lower panel) during the period 3-12 October 1992. Data source:Topex-Poseidon (NASA-CNES) and Jet Propulsion Laboratory.

Cyclones and ocean waves

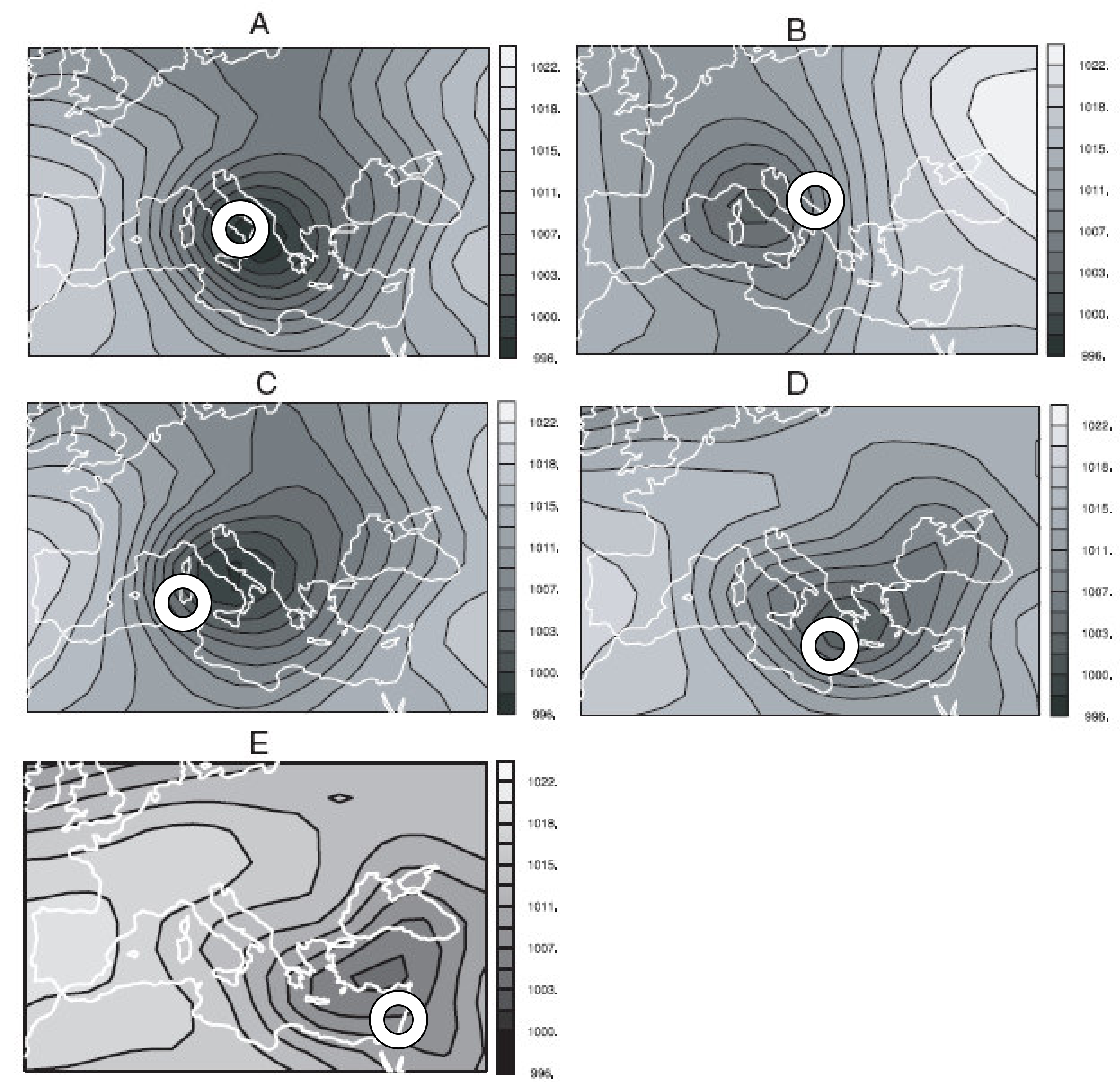

Synoptic patterns associated with extreme significant wave height in different regions of the Mediterranean Sea: a) Tyrrenian b) Adriatic c) Balearic d) Ionian e) Levantine basin (from Lionello et al. 2006)

A deterministic approach to wind wave evolution on oceanic scale is clearly unpractical

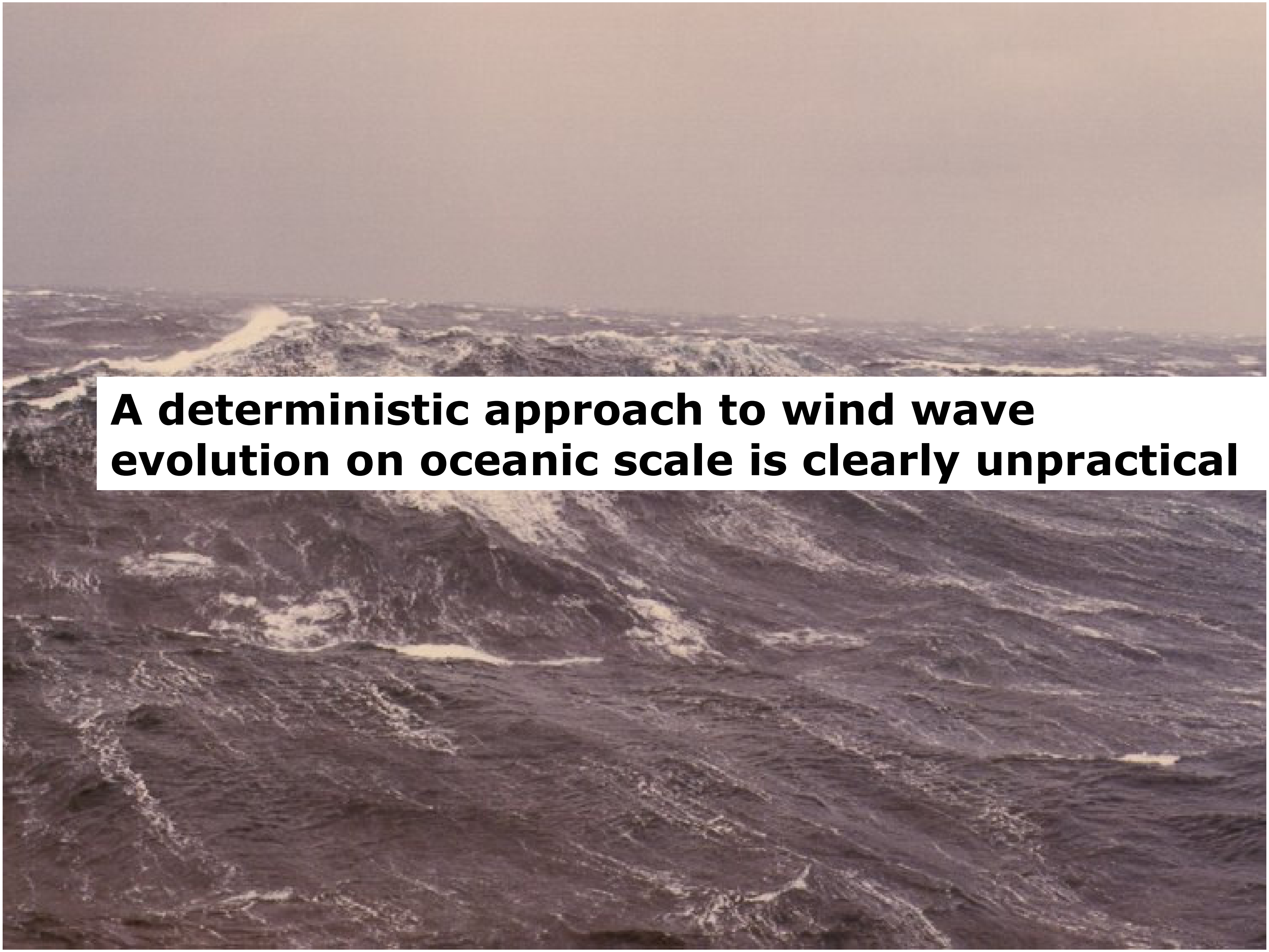

From the Fourier component of the surface elevation

$$\eta(x,t) = \int \hat{\eta}(\vec{k}) e^{i(\vec{k}\vec{x}-\sigma t)} d\vec{k}$$

The wave spectrum is defined as

$$F(\vec{k}_1)\delta(\vec{k}_1 - \vec{k}_2) = < \hat{\eta}(\vec{k}_1)\hat{\eta}^*(\vec{k}_2) >$$

So that

$$< \eta^2(x,t) > = \int F(\vec{k}) d\vec{k}$$

and

$$SWH = \sqrt{4 < \eta^2(x,t) >}$$

Significant wave height is a measure of the observed height and of the wave energy

Wave models are grouped in 0+3 generations:

- generation 0: "Tables" for SWH and f_p

Spectrum: distribution of energy as function of frequency and direction

- generation 1: growth of the spectrum up to a saturation level

- generation 2: Parametric spectral shape which describes overshoot and growth of frequencies that do not receive energy directly from the wind

- generation 3: parameterization of physical processes responsible for the evolution of the spectrum

WAM (Wave Model), WAMDI Group, JPO, 1987

Winslow Homer (1836-1910):
"The Woodlock",
Boston Fine Arts Museums

- generation 0: "Tables" for SWH and f_p

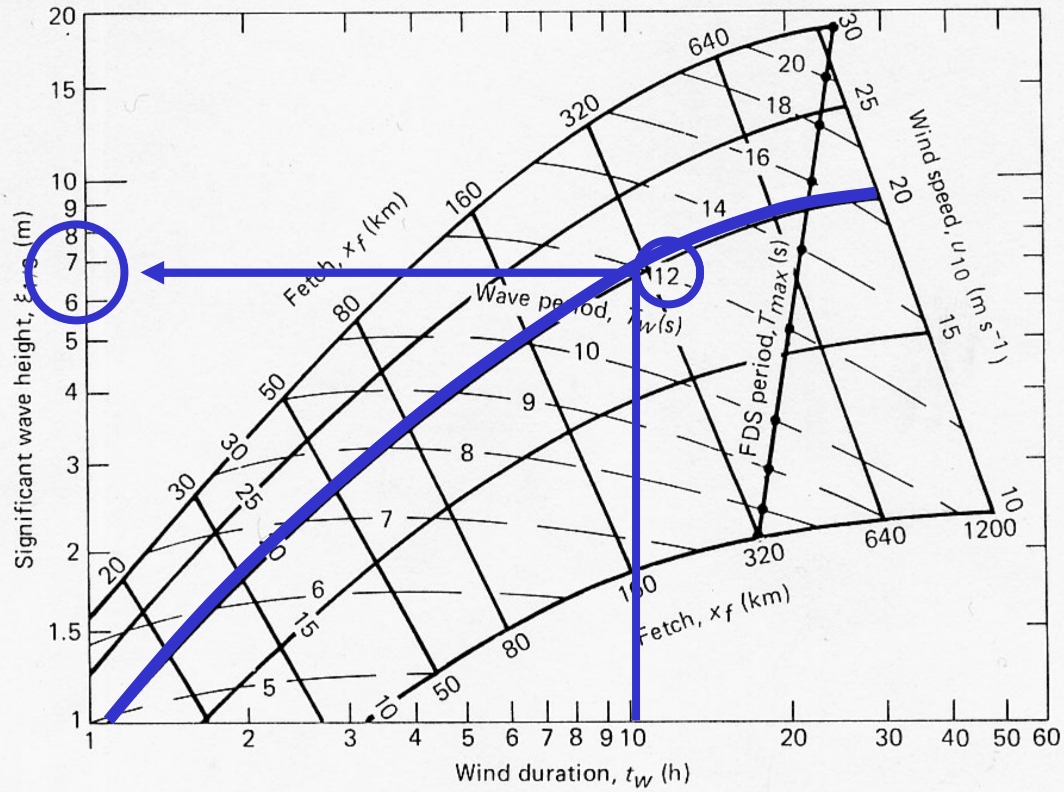

Fig. 5.5 Cumulative sea state diagram showing significant wave height, $\xi_{1/3}$, as a function of wind duration, fetch, and speed. A fully developed sea (FDS) is considered as having arisen from conditions shown along the near vertical line labeled "FDS period, T_{max}." [Adapted from Van Dorn, W. G., *Oceanography and Seamanship* (1974).]

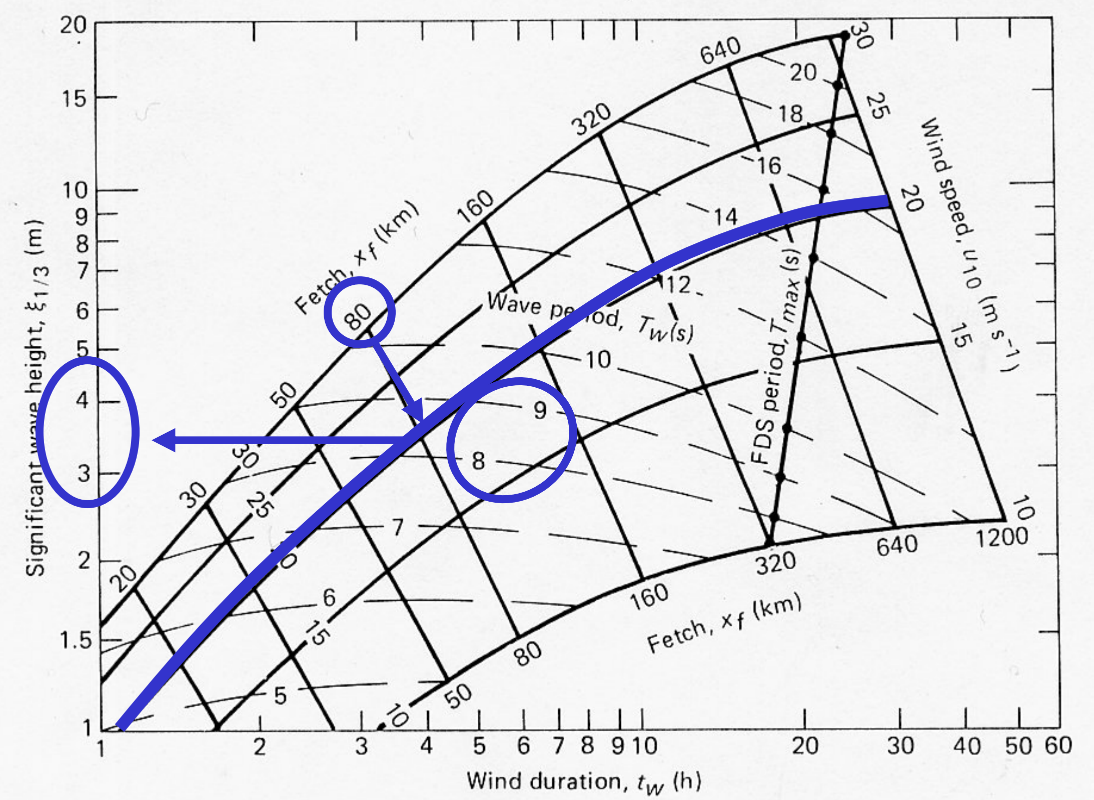

Fig. 5.5 Cumulative sea state diagram showing significant wave height, $\xi_{1/3}$, as a function of wind duration, fetch, and speed. A fully developed sea (FDS) is considered as having arisen from conditions shown along the near vertical line labeled "FDS period, T_{max}." [Adapted from Van Dorn, W. G., *Oceanography and Seamanship* (1974).]

- generation 1:
growth of the spectrum up to a saturation level

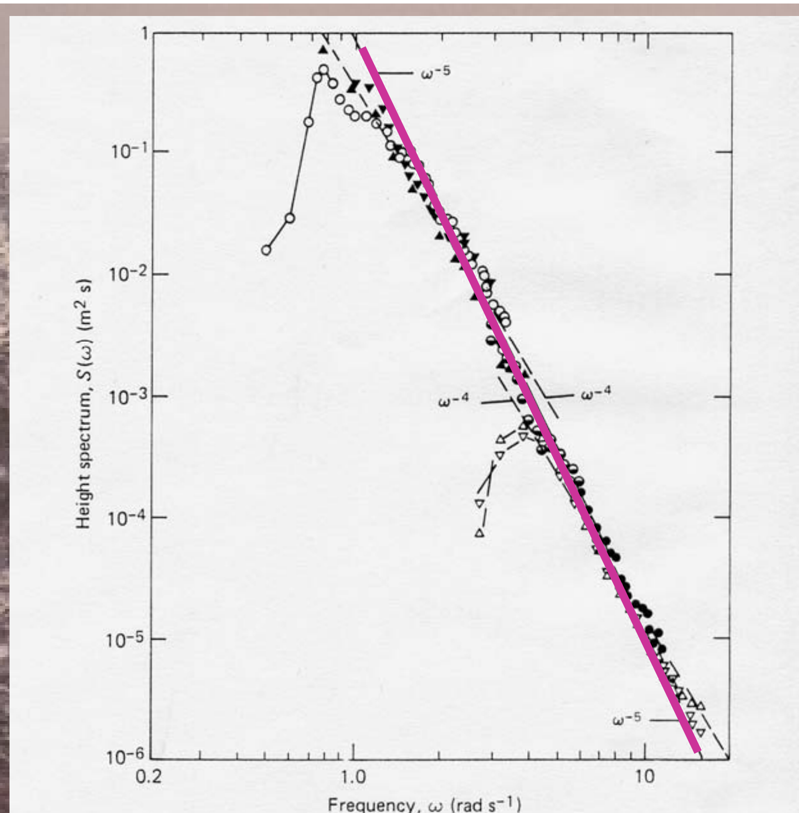

Fig. 5.6 Height spectrum of surface gravity waves as a function of frequency, for the "equilibrium range" beyond the spectral peak; the shape of the peak is shown for only three cases. Slope of the solid straight line is -5 (cf. Eq. 5.109). However, more recent work suggests that the slope of the high-frequency region may actually be -4 if analyzed differently (dashed lines). [Adapted from Phillips, O. M., *The Dynamics of the Upper Ocean* (1977).]

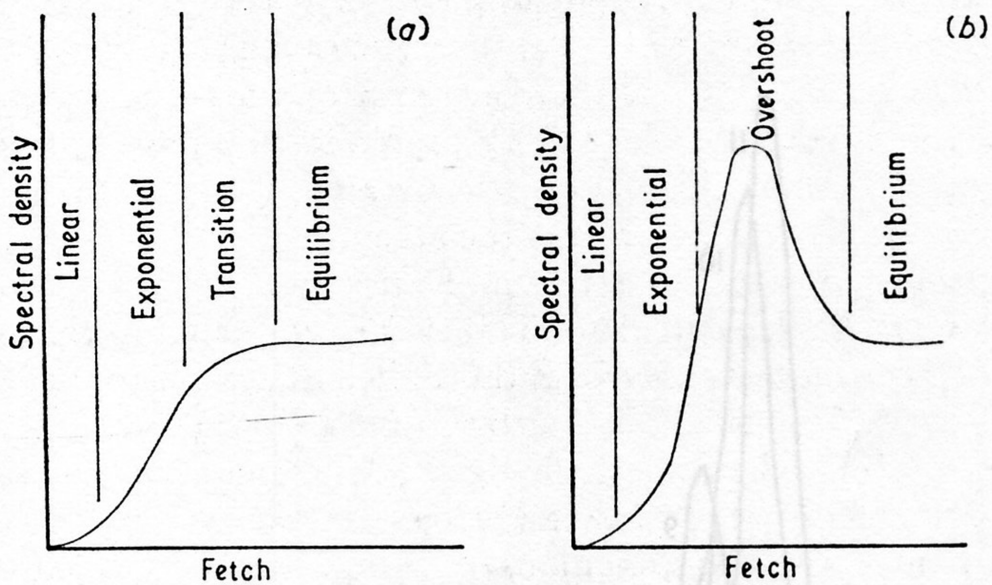

Figure 4. Schematic growth curves for selected frequency component of the wave spectrum. (*a*) Conventional growth curve based on early theories of wave generation, and (*b*) the observed growth curve clearly demonstrating the overshoot effect (after Barnett and Sutherland 1968).

- generazione 2:
Parametric spectral shape which describes overshoot and growth of frequencies that do not receive energy directly from the wind

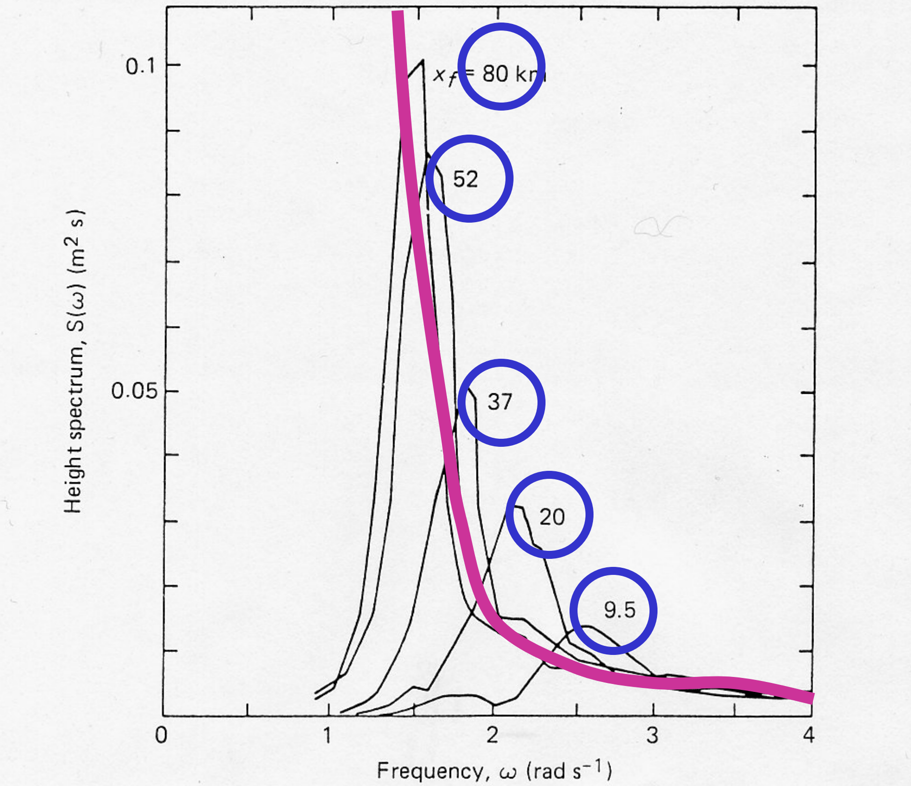

Fig. 5.14 Wind wave spectra for five increasing fetches, x_f. [Adapted from Hasselmann, K., et XV al., *Deutsch. Hydrogr. Z.* (1973).]

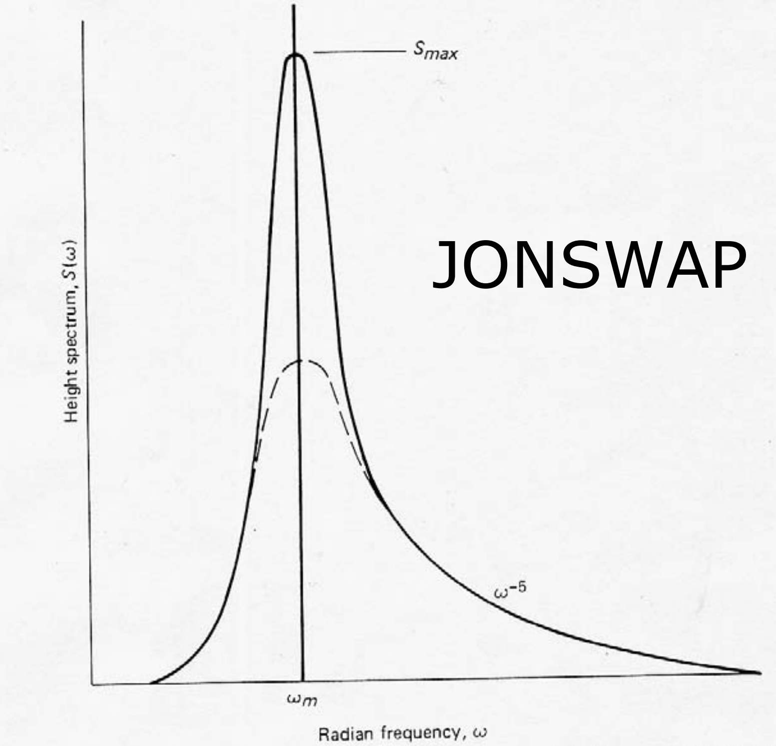

Fig. 5.15 Schematic form of JONSWAP semiempirical wind wave spectrum. The dotted line gives the Pierson–Moskowitz spectral shape, for which Fourier components are essentially independent; the solid line is more peaked due to nonlinear interactions. [Adapted from Hasselmann, K., et XV al., *Deutsch. Hydrogr. Z.* (1973).]

- Generation 3: parameterization of physical processes responsible for the evolution of the spectrum

$$\boxed{\frac{\partial F}{\partial t}} + \boxed{\nabla (C_g F)} = \boxed{S_{in}} + \boxed{S_{nl}} + \boxed{S_{ds}} + \boxed{S_{bf}}$$

Local Variation of the spectrum F

Divergence of the energy flux

Source function

S_{in}: Wind input

S_{nl}:nonlinear interactions

S_{ds}:dissipation

S_{bf}:bottom friction

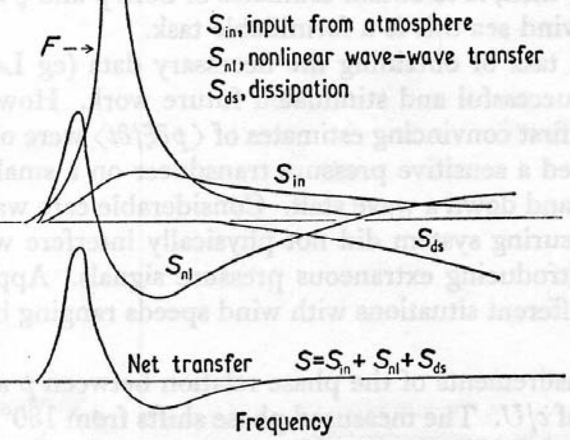

Figure 8. Schematic energy balance for the case of negligible dissipation in the main part of the spectrum from the JONSWAP.

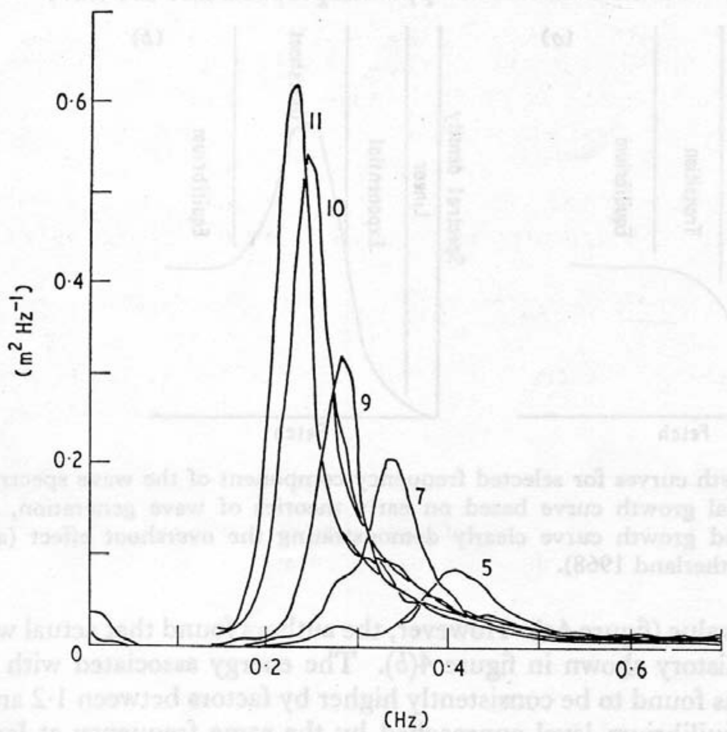

Figure 6. Evolution of the wave spectrum with fetch for offshore wind. Numbers refer to JONSWAP stations at which measurements were made (see figure 5).

Which tools are available for evaluating SWH climate trends

Wave buoys

Unfortunately time series are too sparse (and actually rather short)

Satellite observations

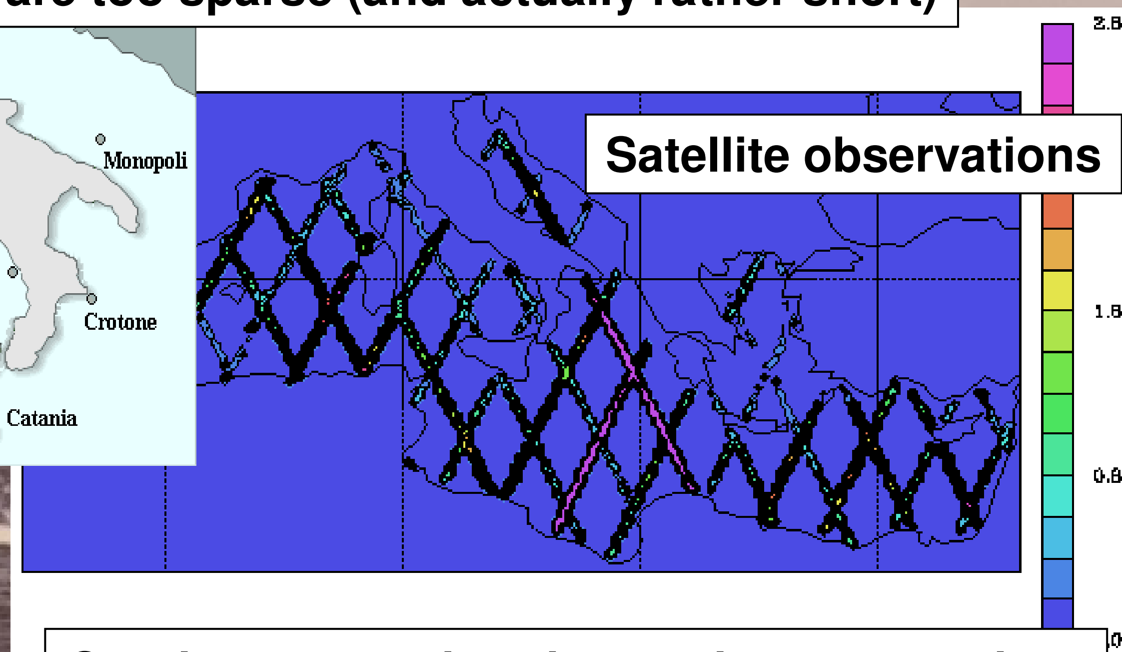

Good coverage, but time series are too short

Reconstruction based on numerical simulations

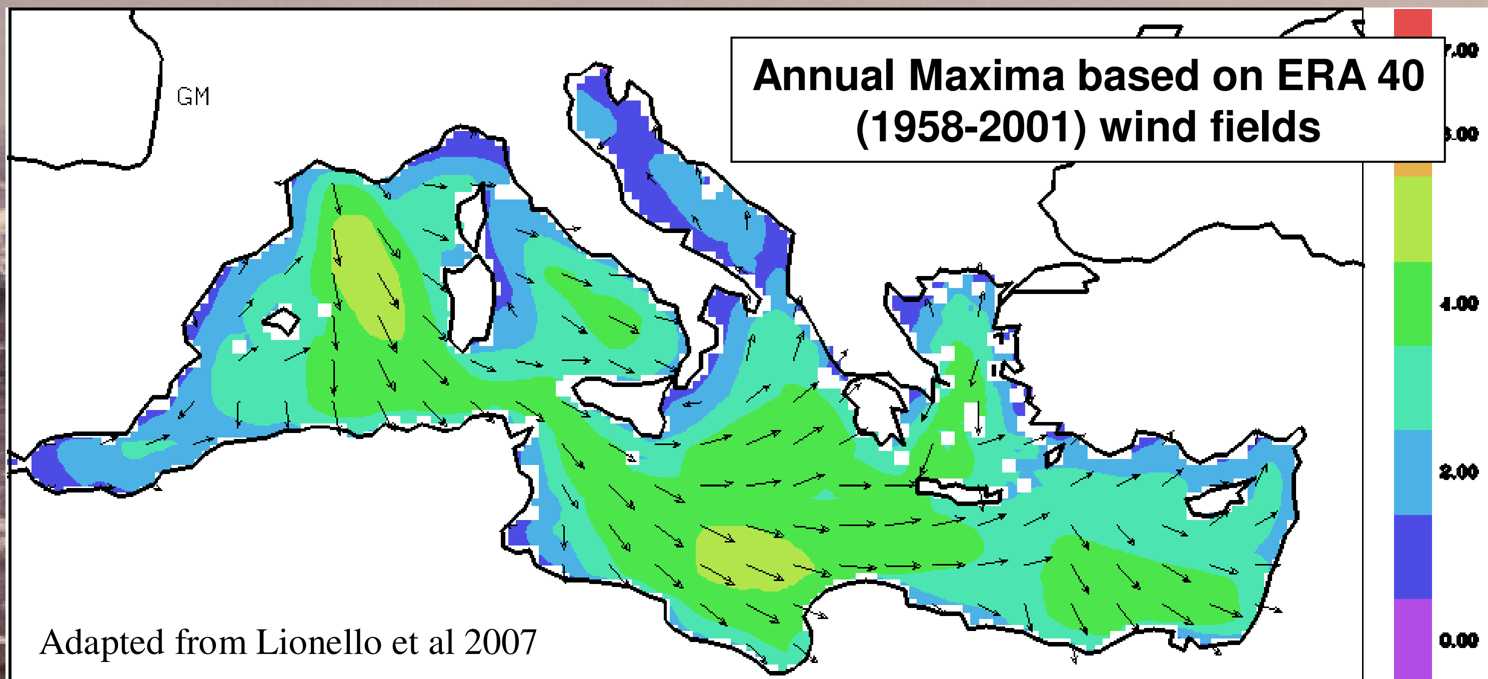

Adapted from Lionello et al 2007

Quality of results is critically depending on wind fields

Model validation

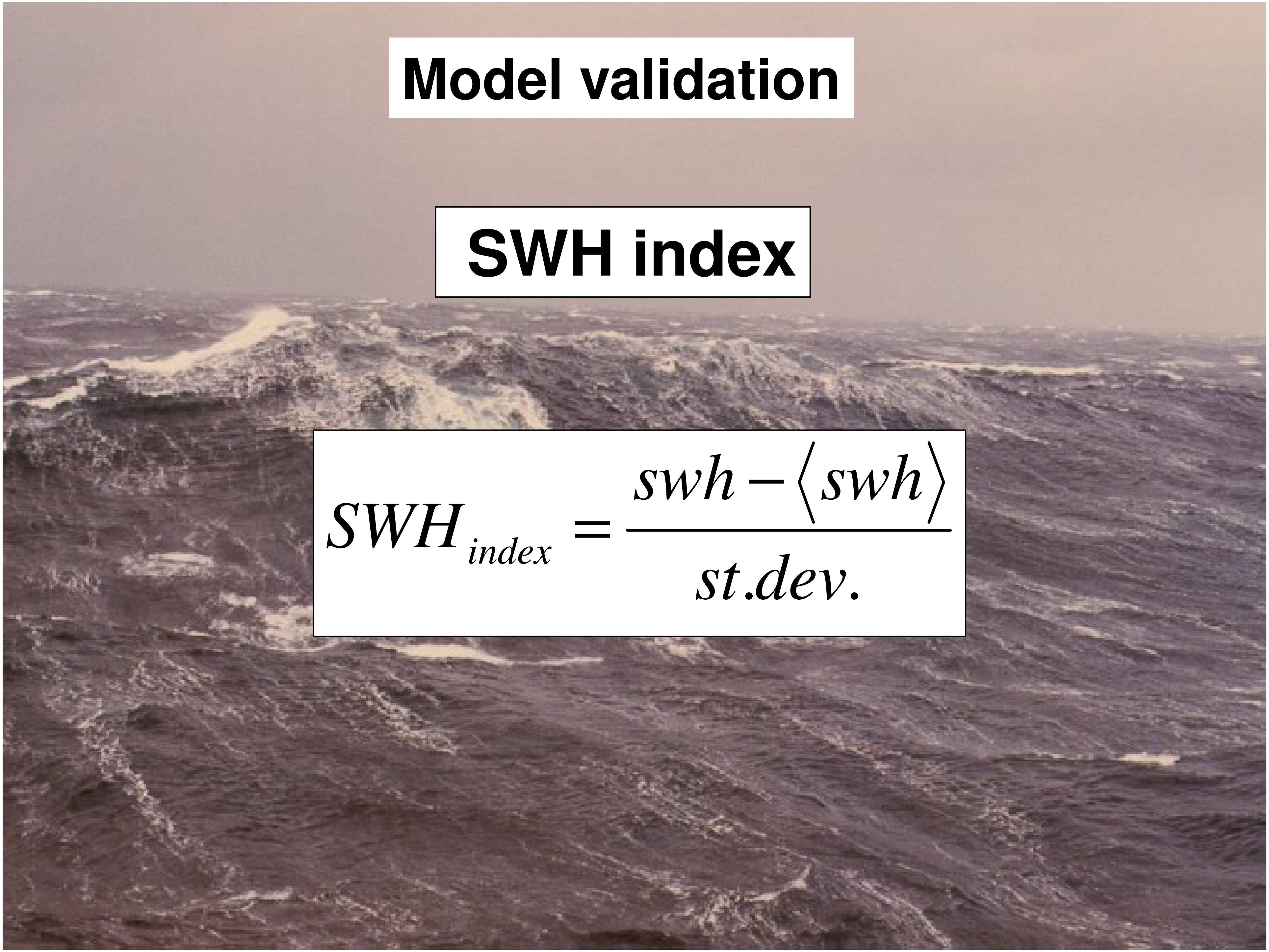

SWH index

$$SWH_{index} = \frac{swh - \langle swh \rangle}{st.dev.}$$

Model validation

correlazione ERA 40-T213 = .88
correlazione ERA 40-RON = .84
correlazione RON-T213 = .86

Buoys

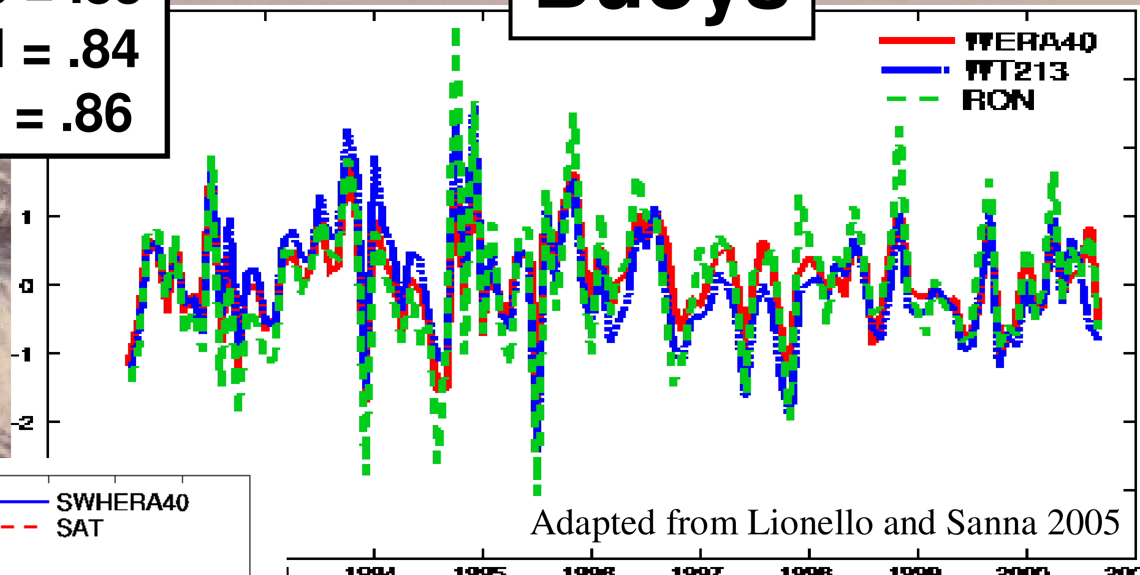

Adapted from Lionello and Sanna 2005

Satellite

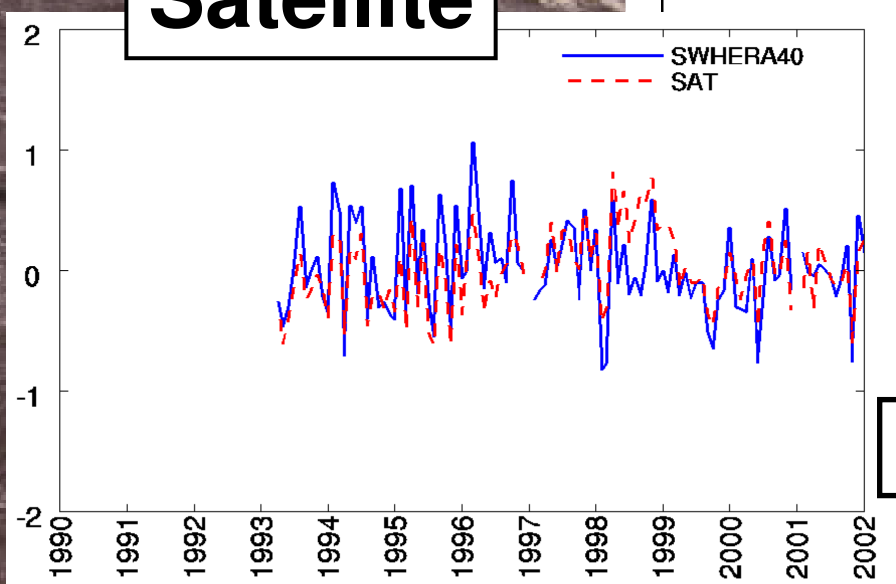

correlazion ERA 40 – SAT = .72

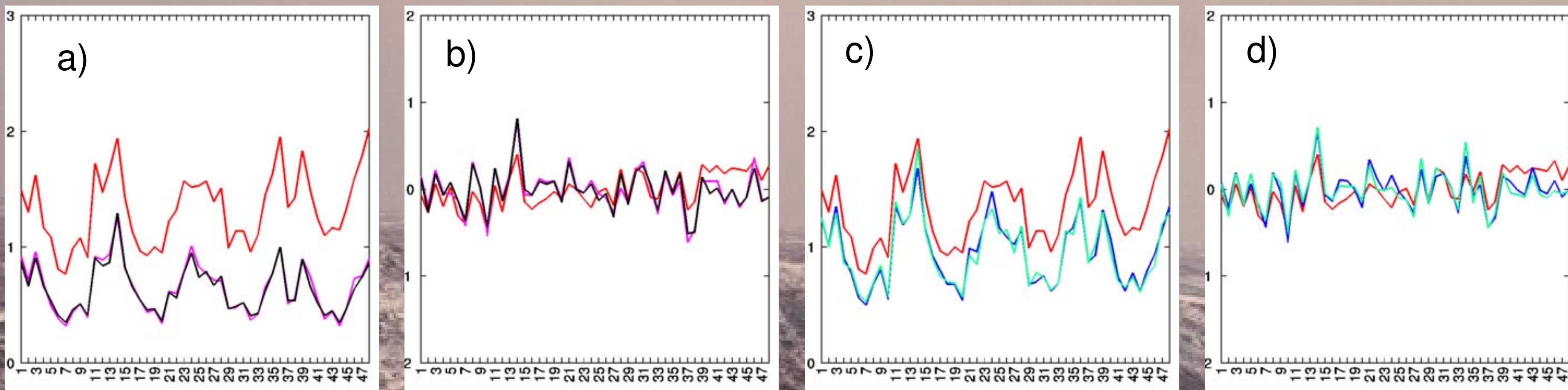

.Panel a) Comparison between monthly average SWH for WAM-ERA40 (black), WW3-ERA40 (pink) modelling configuration and satellite data (red).
Panel b): same as panel a), except it shows the dimensionless index.
Panel c) Same as panel a), except it shows the model results with HIPOCAS forcing.
Panel d) Same as panel c), except it shows the model results with HIPOCAS forcing (green and blue line for WAM and WW3 models, respectively).
Values in meters (y-axis), calendar months on the x axis.

From Galati et al, 2008

AVERAGE SWH						DIMENSIONLESS INDEX
Model-Wind	**Satellite Average**	**Standard Deviation**	**Model Average**	**Standard Deviation**	**Correlation**	**Correlation**
WAM-ERA40	1.34	0.31	0.64	0.21	0.87	0.61
WAM-HIPOC	1.34	0.31	0.96	0.29	0.90	0.68
WW3-ERA40	1.34	0.31	0.65	0.23	0.88	0.61
WW3-HIPOC	**1.34**	**0.31**	**0.96**	**0.29**	**0.91**	**0.71**

Average SWH and dimensionless index for each configuration and for satellite data, their standard deviation and correlation (SWH values in meters).

Adapted from Galati et al, 2008

Scatter plot for the modeling configurations

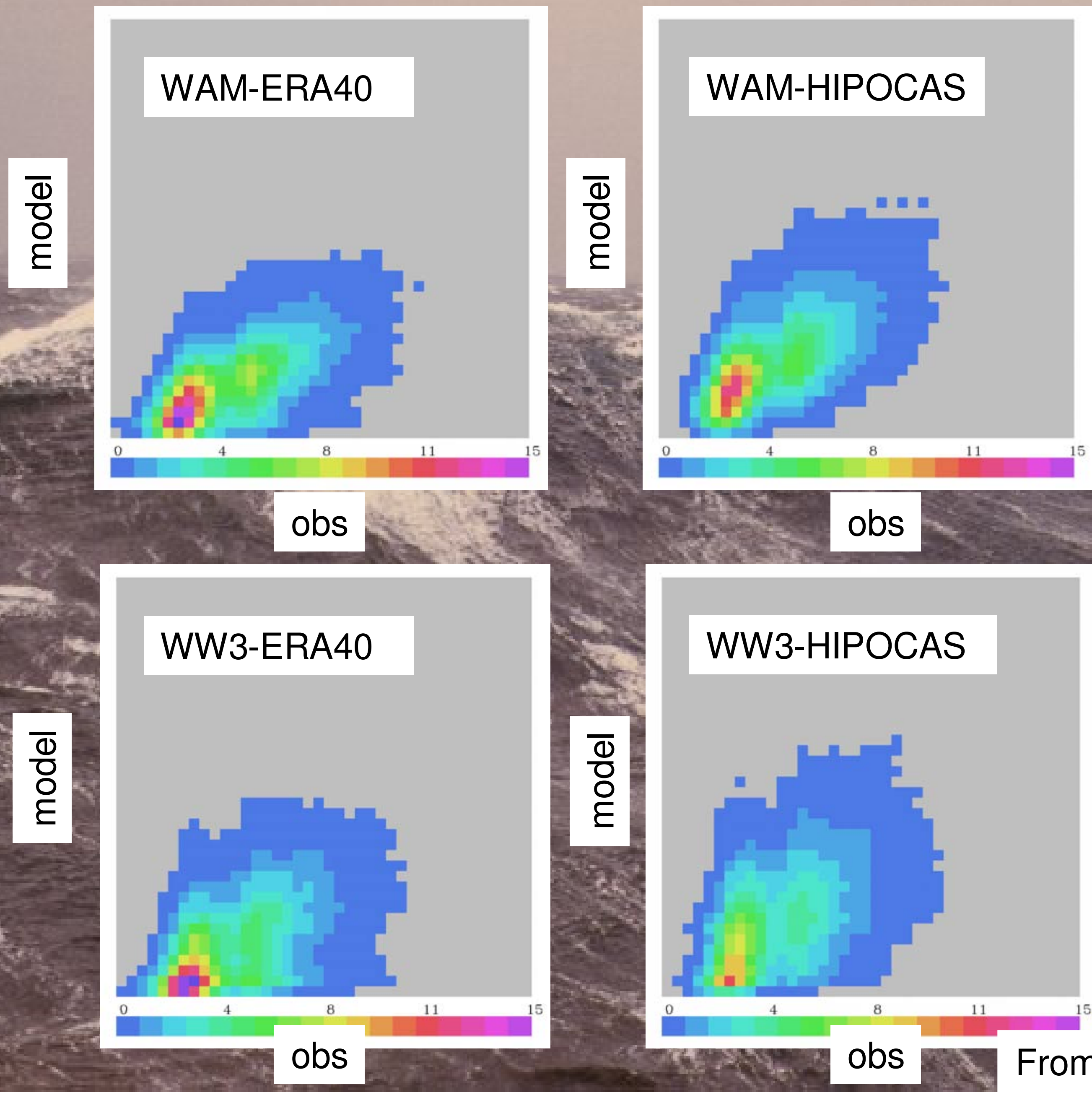

From Galati et al, 2008

Present trends

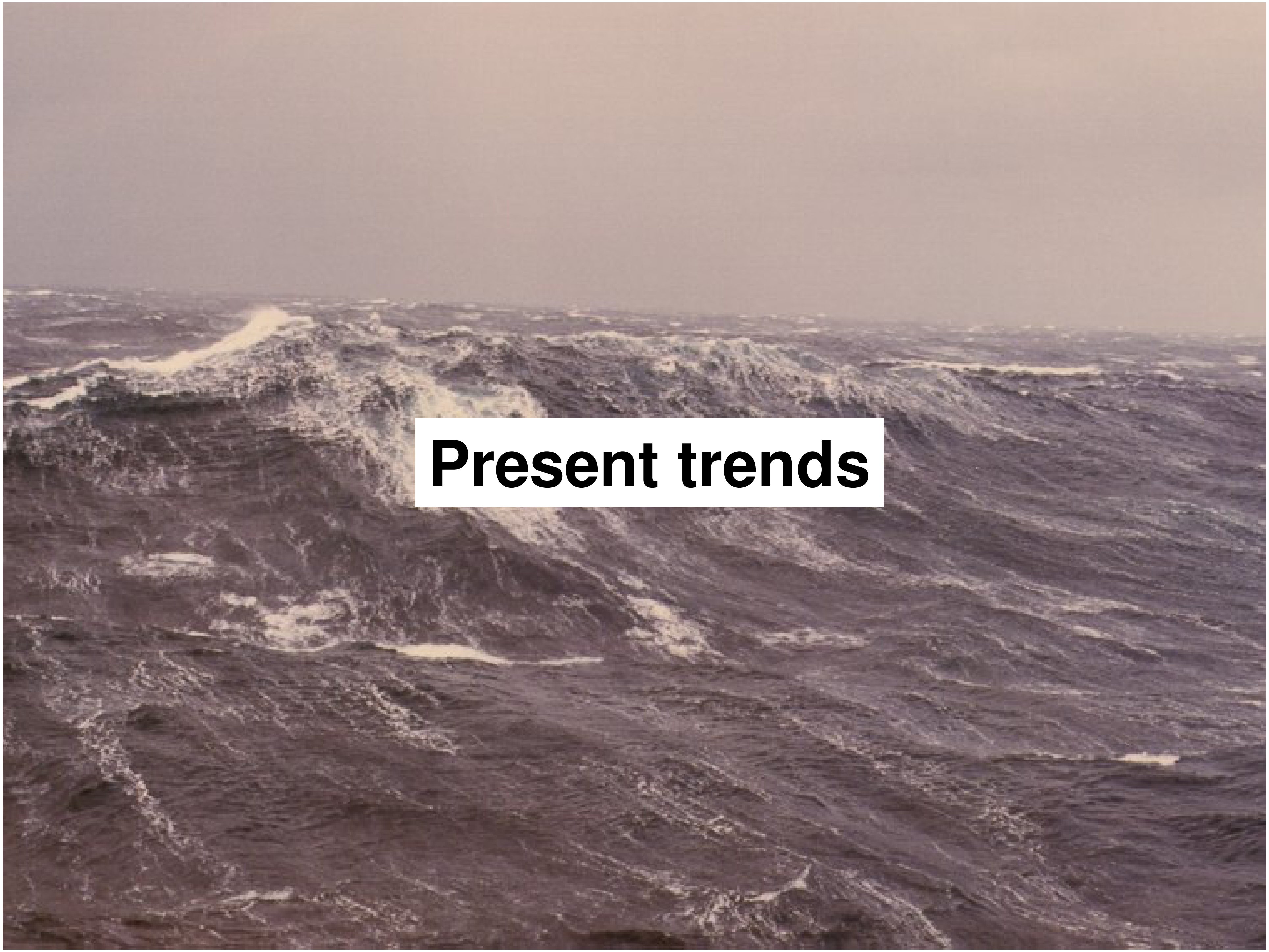

Tendenze dell'attività ciclonica nella seconda metà del 20º secolo

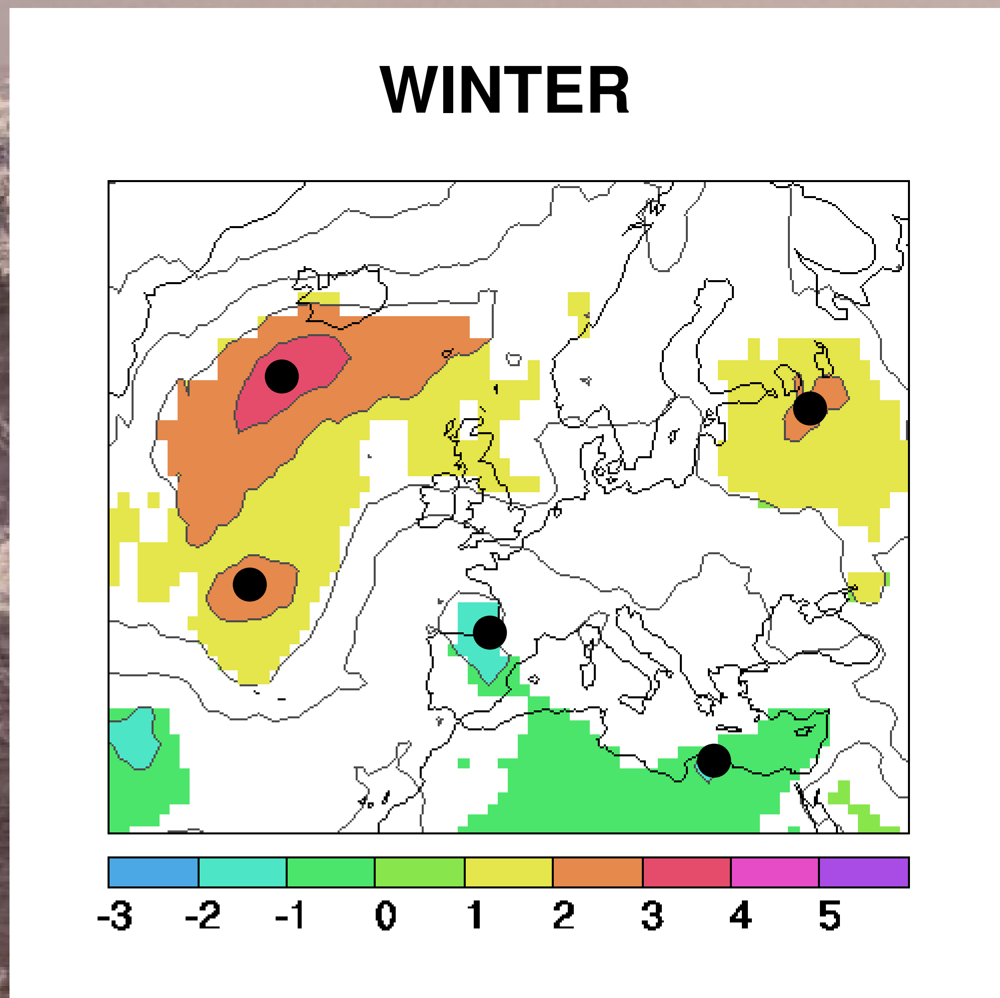

Mean SWH: present trends

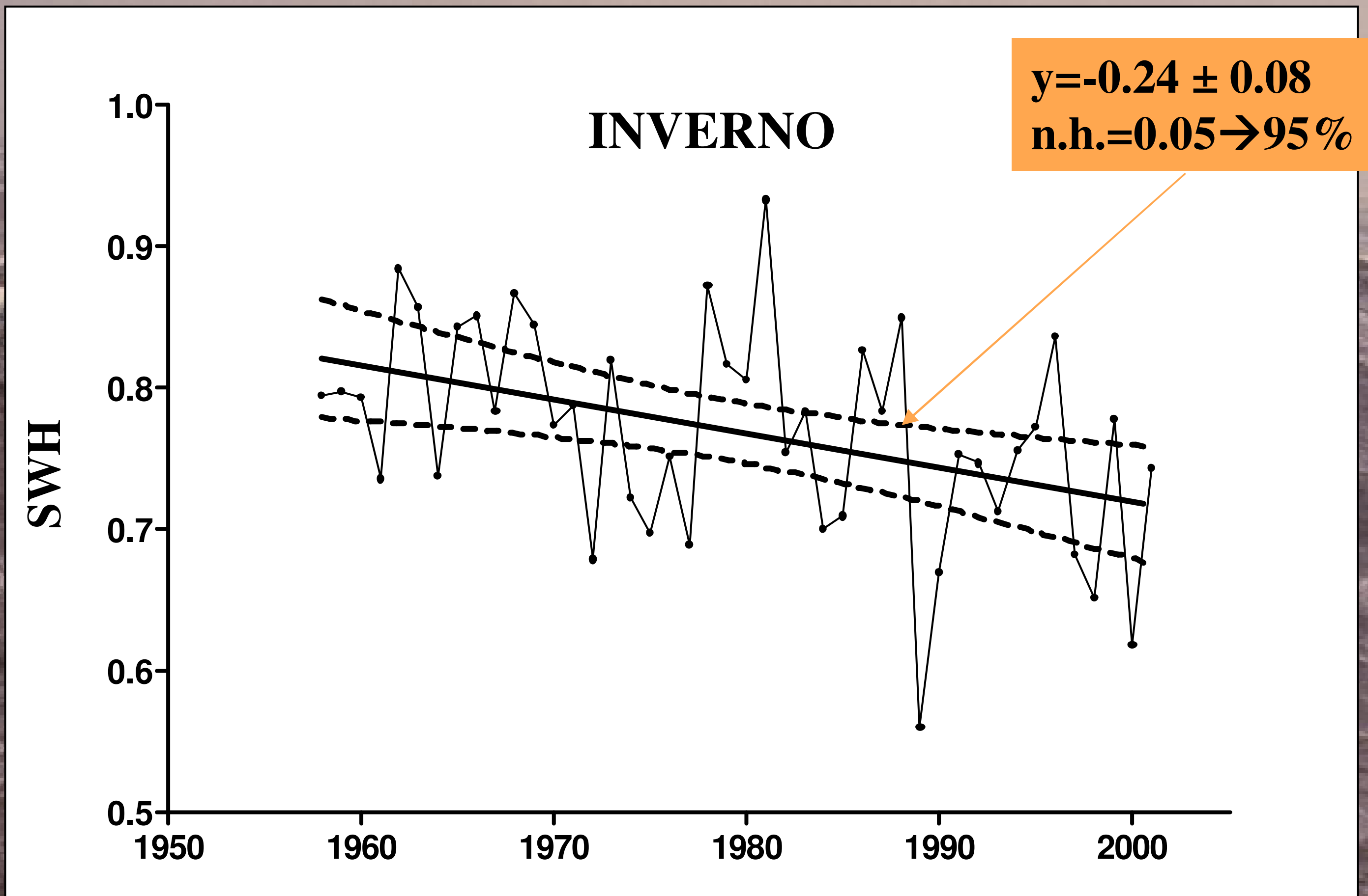

From Lionello and Sanna 2005

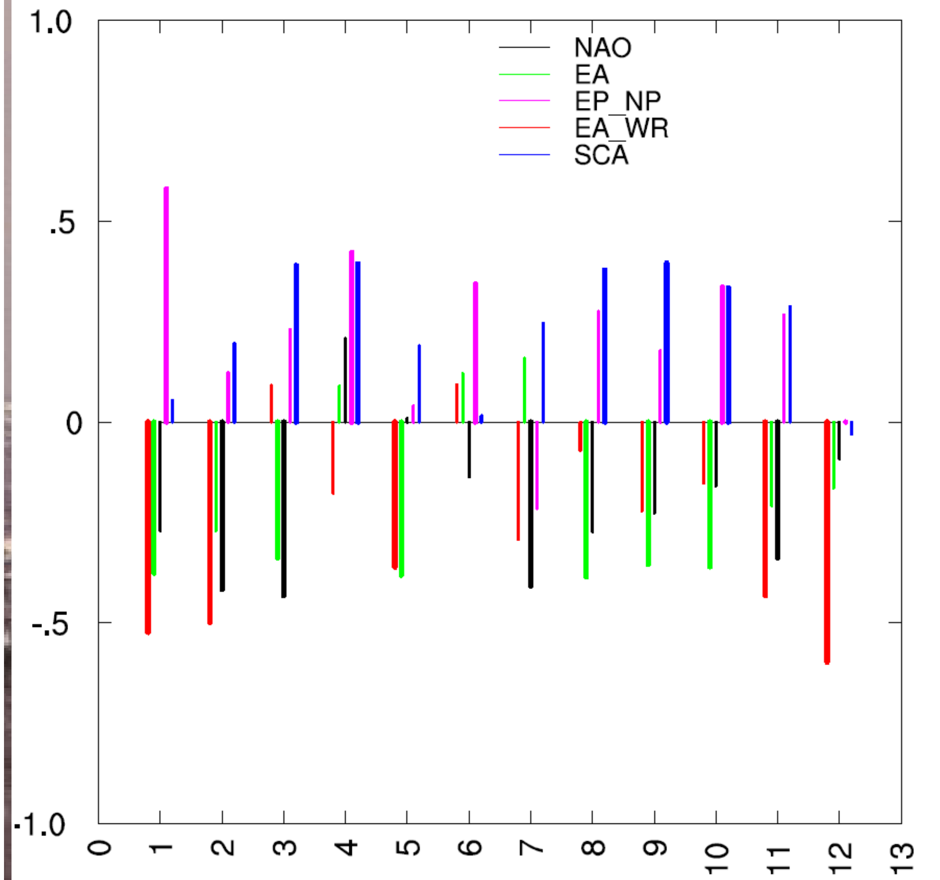

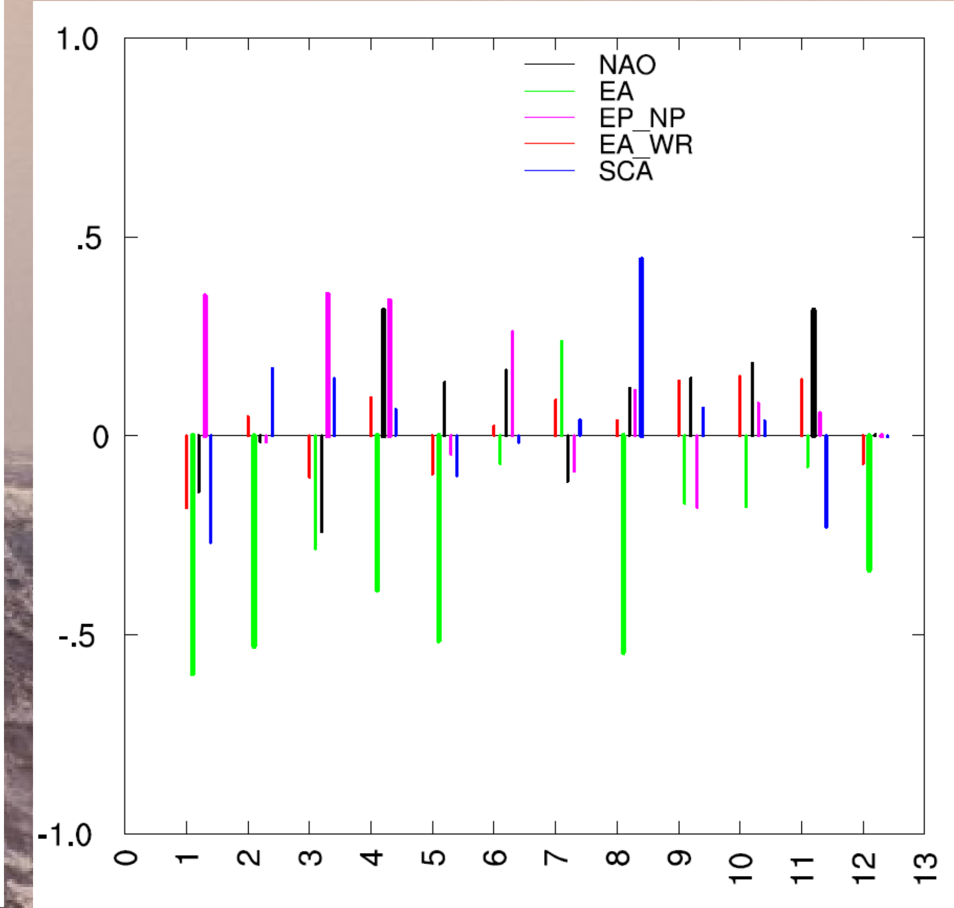

Annual cycle (calendar months on the x-axis) of the correlation between monthly average SWH field and teleconnection pattern indexes. Only NAO, EA, EP/NP, EA/WR, SCA are shown. Other patterns have smaller and less relevant correlation values. Thick bars denote value significant at the 95% confidence level. The two panels refer to the western (top) and eastern (bottom) part of the Mediterranean.

From Lionello and Galati 2007

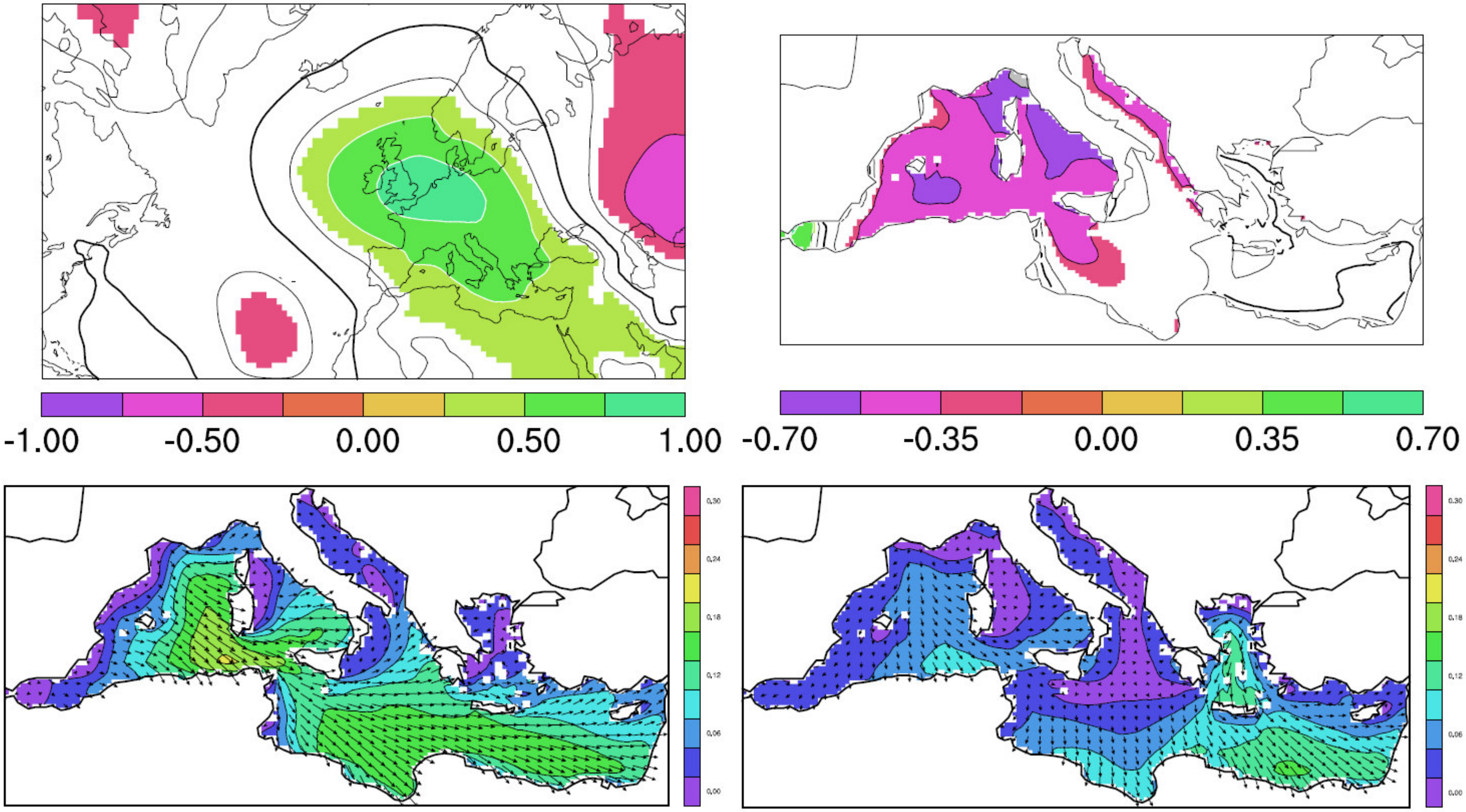

January: correlation of EA-WR index with SLP and SWH, **(a)** and **(b)** panel, respectively. In the color filled areas the correlation is significant at the 95% confidence level. Panels **(c)** and **(d)** composites of SWH (meters) during months with the 9 most high and low values of the EA-WR index, respectively.

From Lionello and Galati 2007

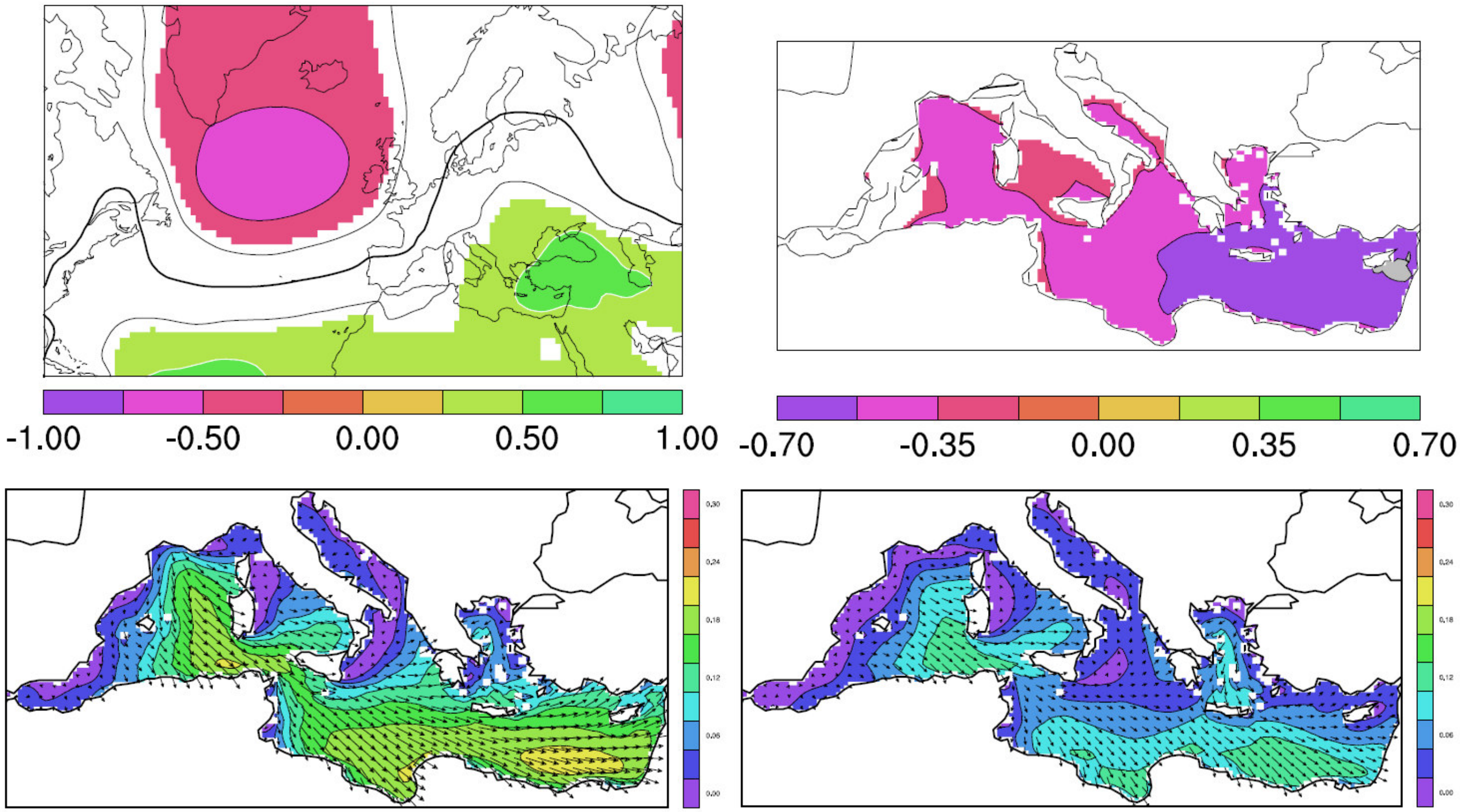

Fig. 2. January: correlation of EA index with SLP and SWH, **(a)** and **(b)** panel, respectively. In the colour filled areas the correlation is significant at the 95% confidence level. Panels **(c)** and **(d)** composites of SWH (meters) during months with the 9 most high and low values of the EA index, respectively.

January: correlation of EA index with SLP and SWH, **(a)** and **(b)** panel, respectively. In the color filled areas the correlation is significant at the 95% confidence level. Panels **(c)** and **(d)** composites of SWH (meters) during months with the 9 most high and low values of the EA index, respectively.

From Lionello and Galati 2007


Climate change

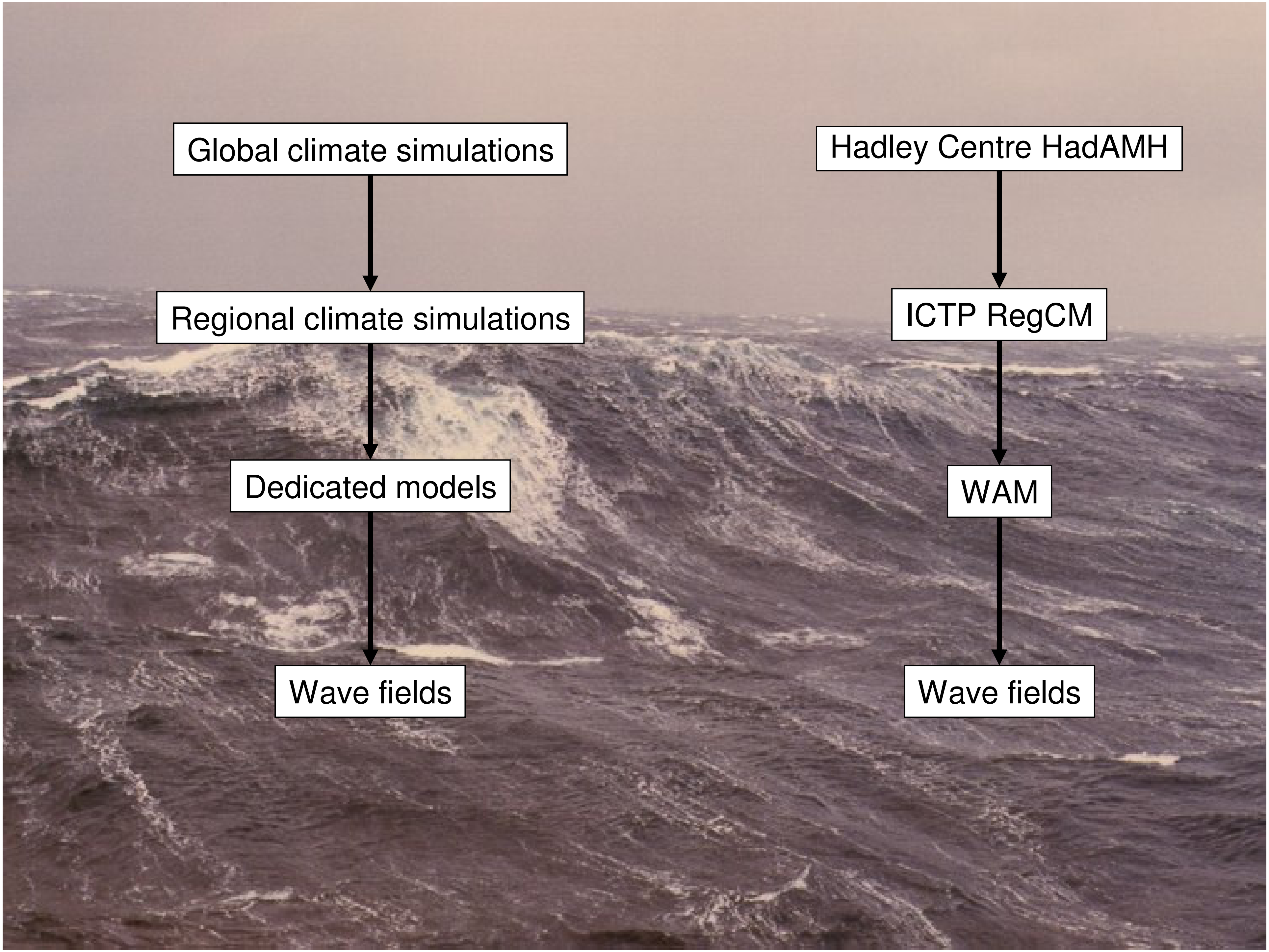
Global climate simulations
Regional climate simulations
Dedicated models
Wave fields
Hadley Centre HadAMH
ICTP RegCM
WAM
Wave fields

RegCM experiment design

Giorgi, F., X. Bi and J.S. Pal , 2004 a and b

- Global Model: Hadley Centre HadAMH
  - Dx = 1.25 lat x 1.875 lon
  - SST from HadCM3 run
  - Coupled sulfur model
- Regional model: ICTP RegCM
  - Dx = 50 km
  - SST, GHG and sulfate from HadAMH
  - aerosol effects
- Simulation periods
  - 1961-1990 : Reference run
  - 2071-2100 : Scenario run
- Scenarios: A2, B2

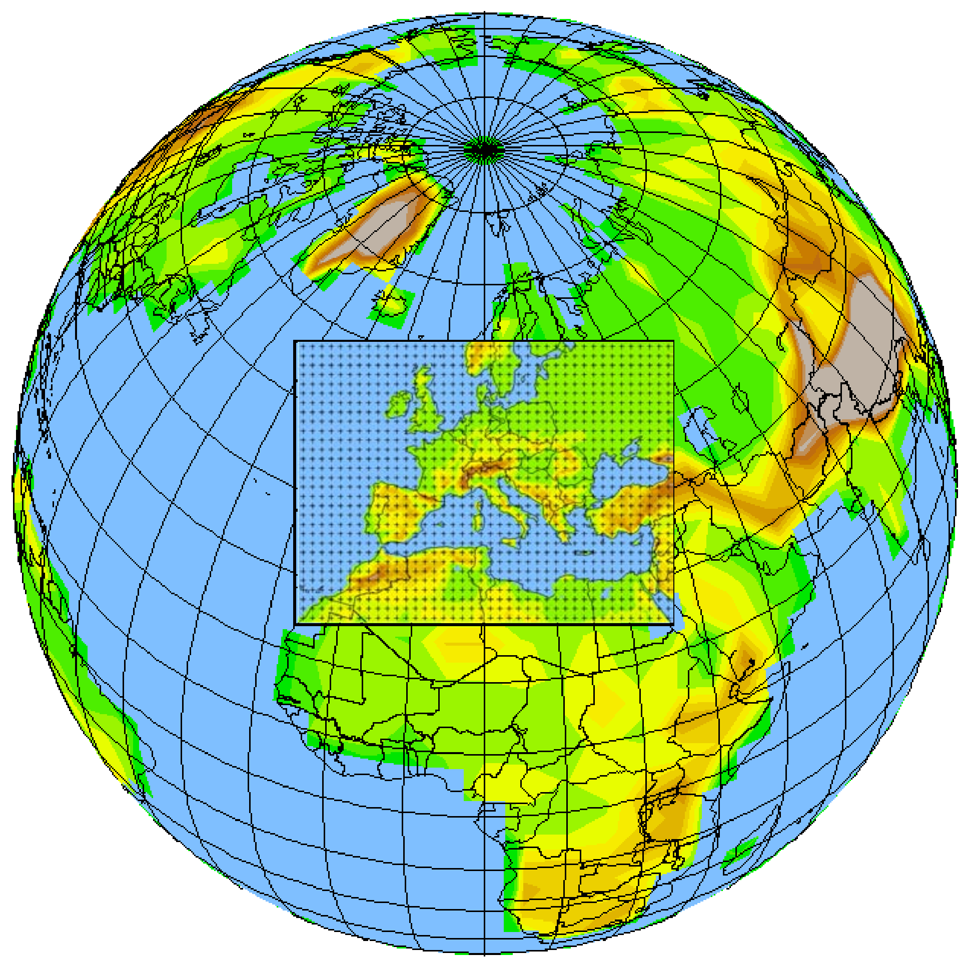

Results are based on 30-year long simulations of the wind-wave field in the Mediterranean Sea carried out with the WAM model.

Wave fields have been computed for 2071-2100 period of the A2, B2 emission scenarios and for 1961-1990 period of the present climate (REF).

The wave model has been forced by the wind field computed by the RegCM regional climate model at a 50km resolution

REF simulation: Comparison between satellite data and model results. Annual cycles are plotted separately for each decade of the simulation. Vertical bars show the standard deviation. Values in meters.

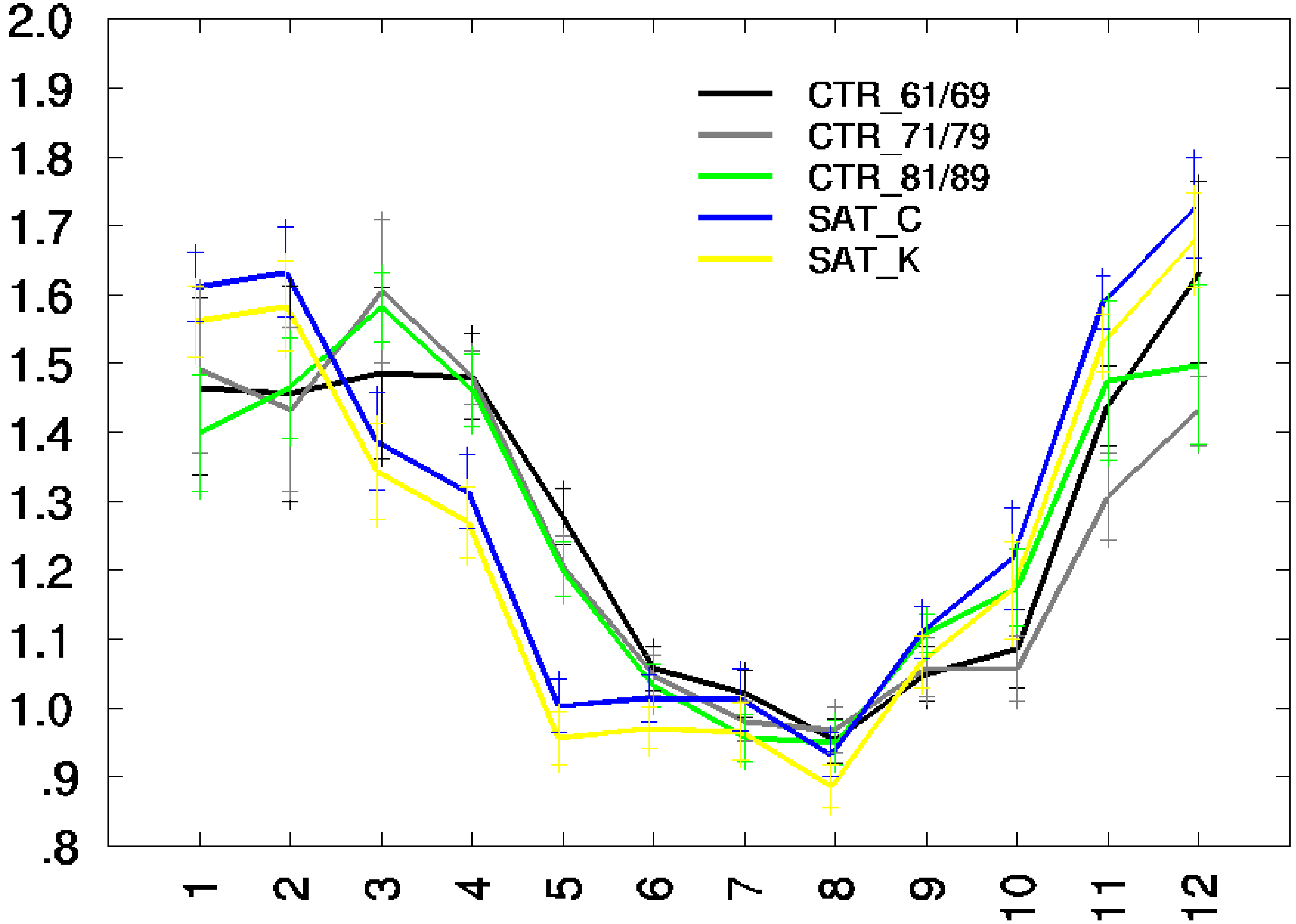

From Lionello et al 2008

Annual average SWH field (metres),

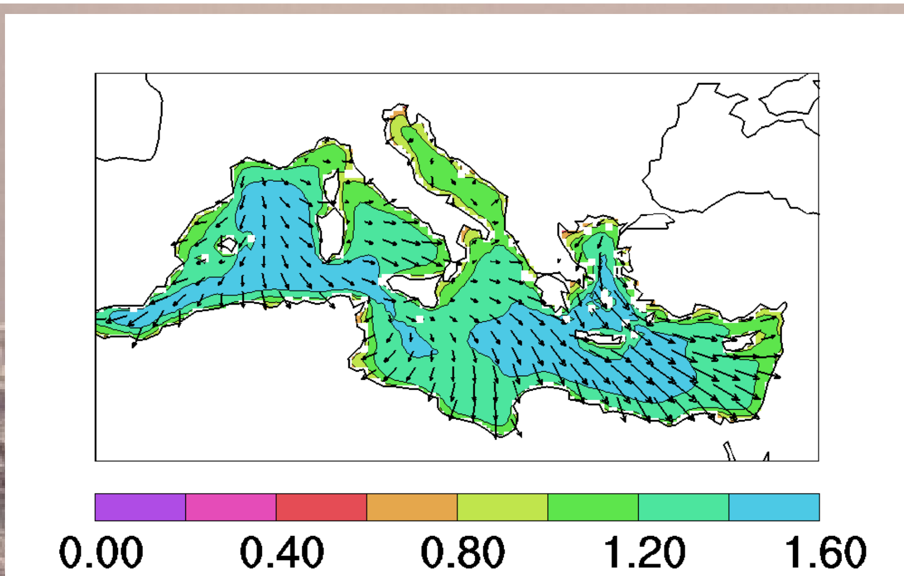

EOFs are normalized with their maximum absolute value

1st EOF

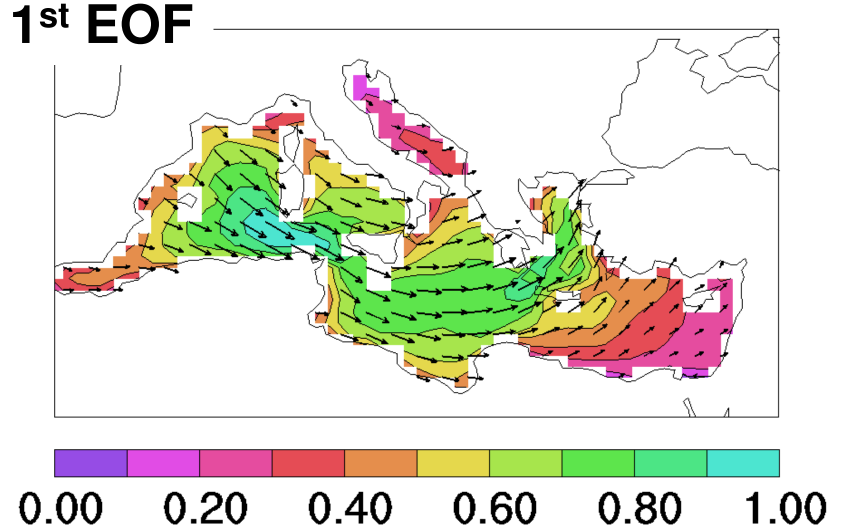

2nd EOF

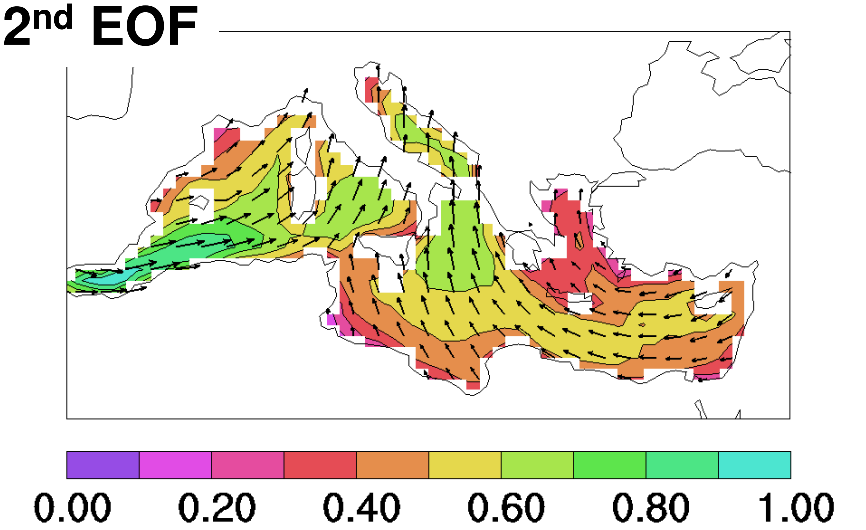

From Lionello et al 2008

average SWH of REF, A2 and B2 scenario simulations

mean annual cycle; vertical bars show the monthly standard deviation (in meters)

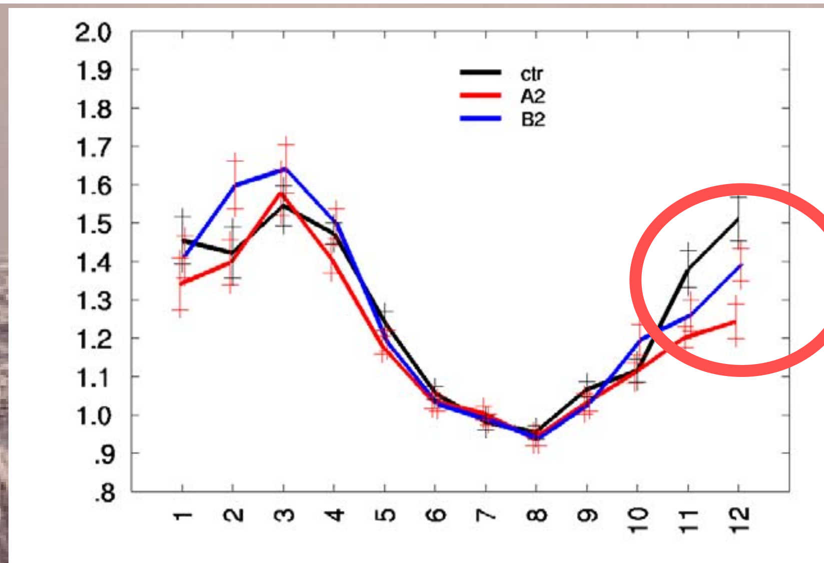

single monthly values (in metres).

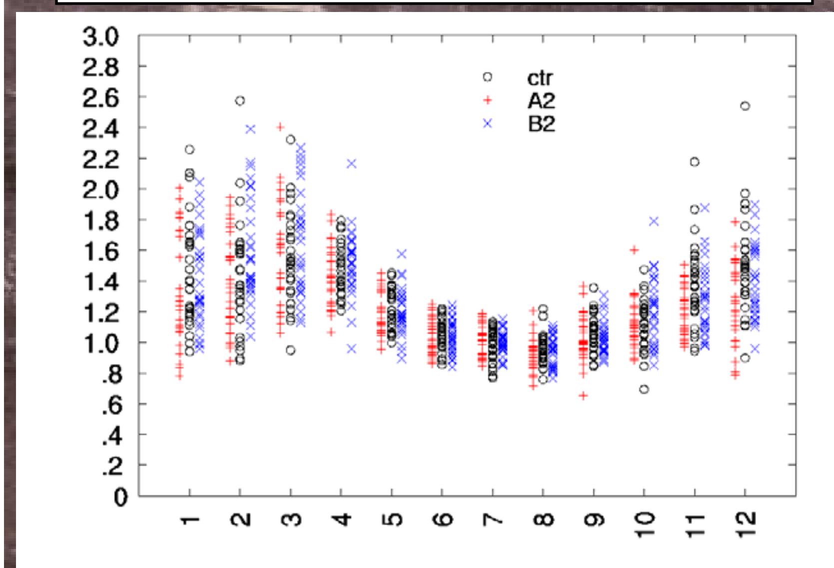

Mann-Whitney test: ranks)

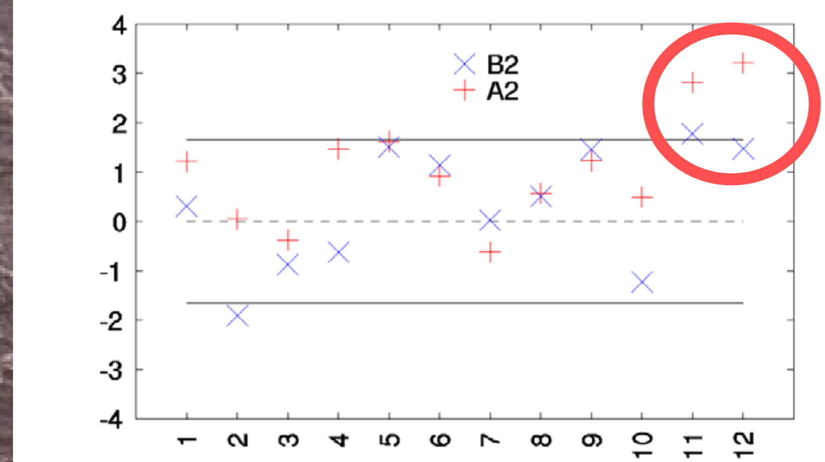

From Lionello et al 2008

1st PC

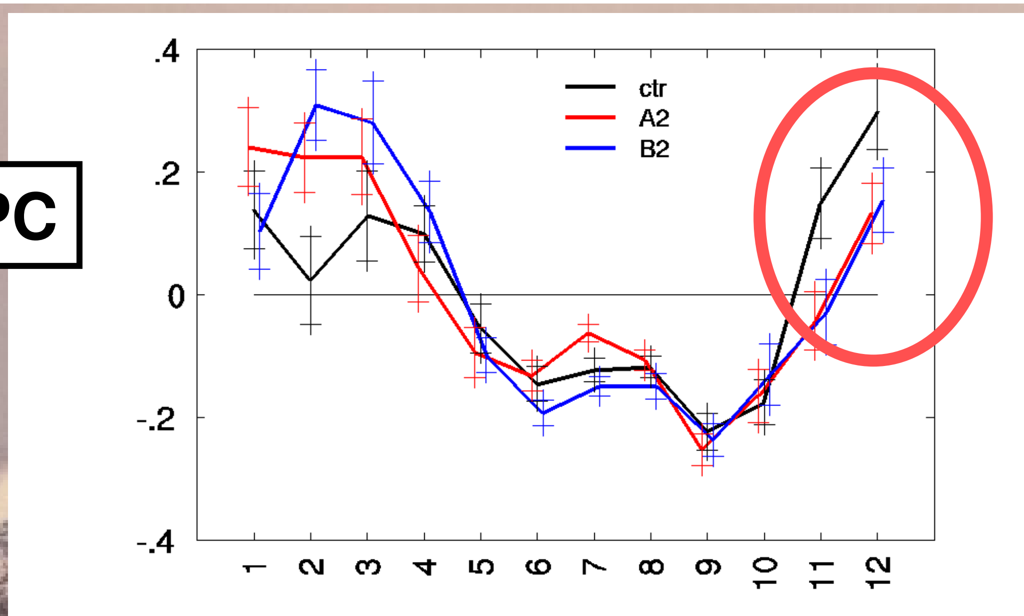

2nd PC

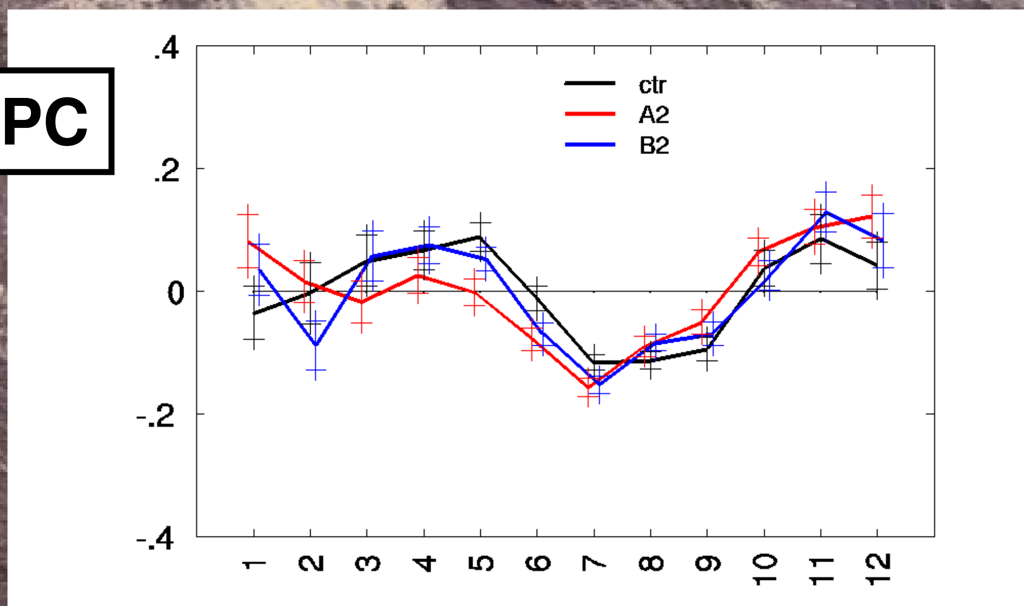

Annual cycle of monthly average values of first (upper panel) and second (lower panel) principal components for REF, A2 and B2 a simulations. Vertical bars show the standard deviation. Values in metres.

SEASONAL MEAN SWH FIELDS

WINTER

From Lionello et al 2008

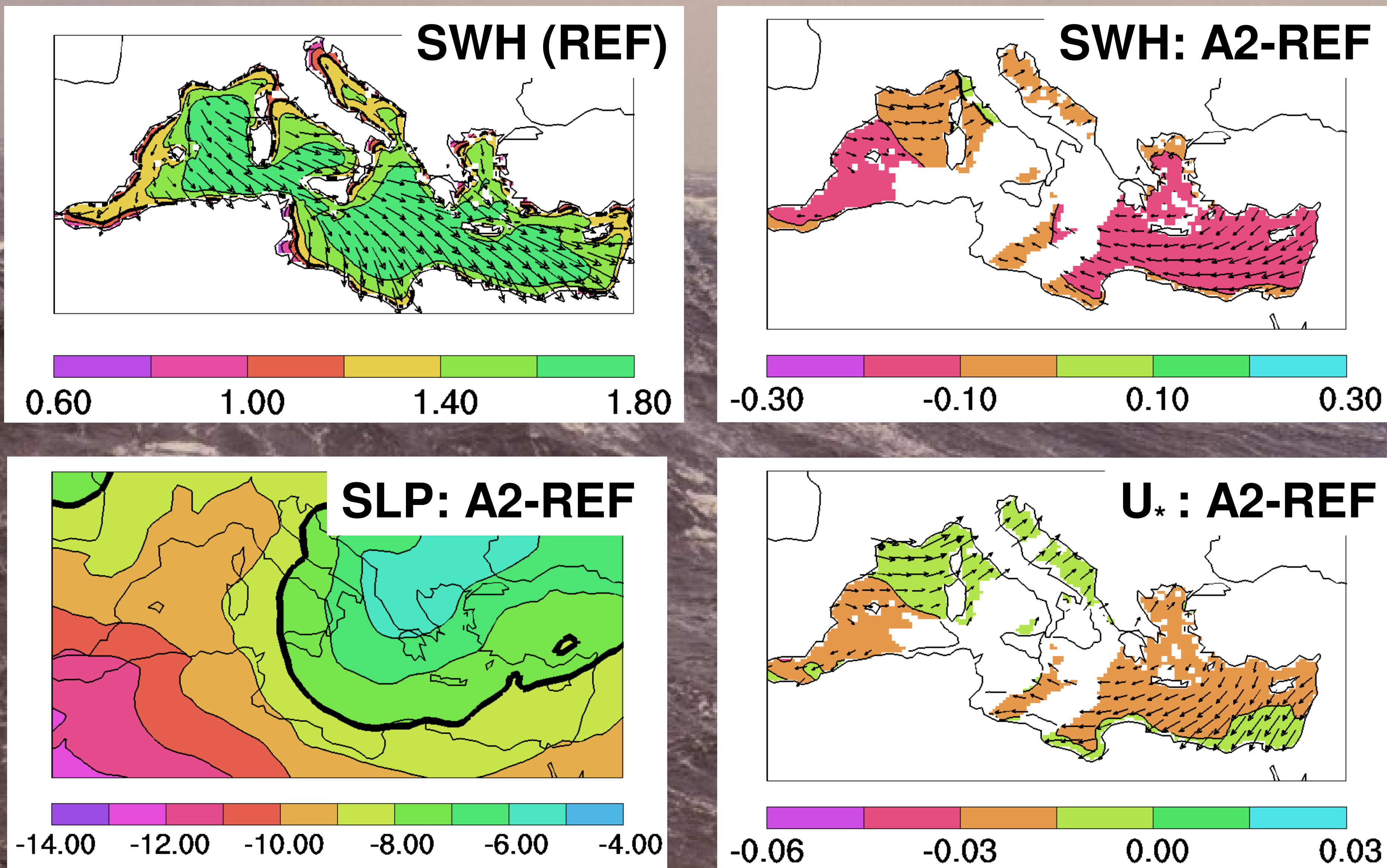

SPRING

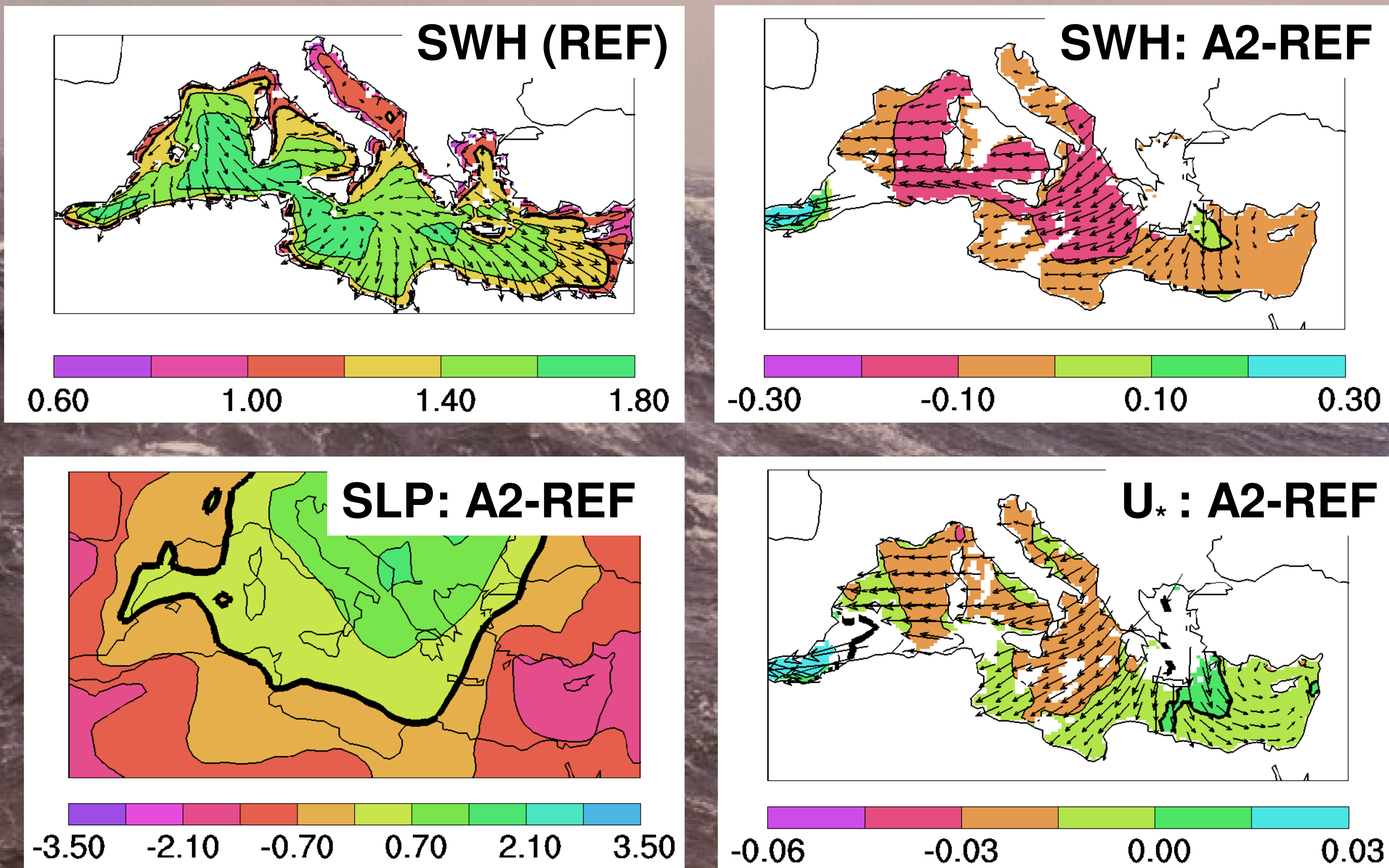
SWH (REF)
0.60
1.00
1.40
1.80
SWH: A2-REF
-0.30
-0.10
0.10
0.30
SLP: A2-REF
-3.50
-2.10
-0.70
0.70
2.10
3.50
U* : A2-REF
-0.06
-0.03
0.00
0.03

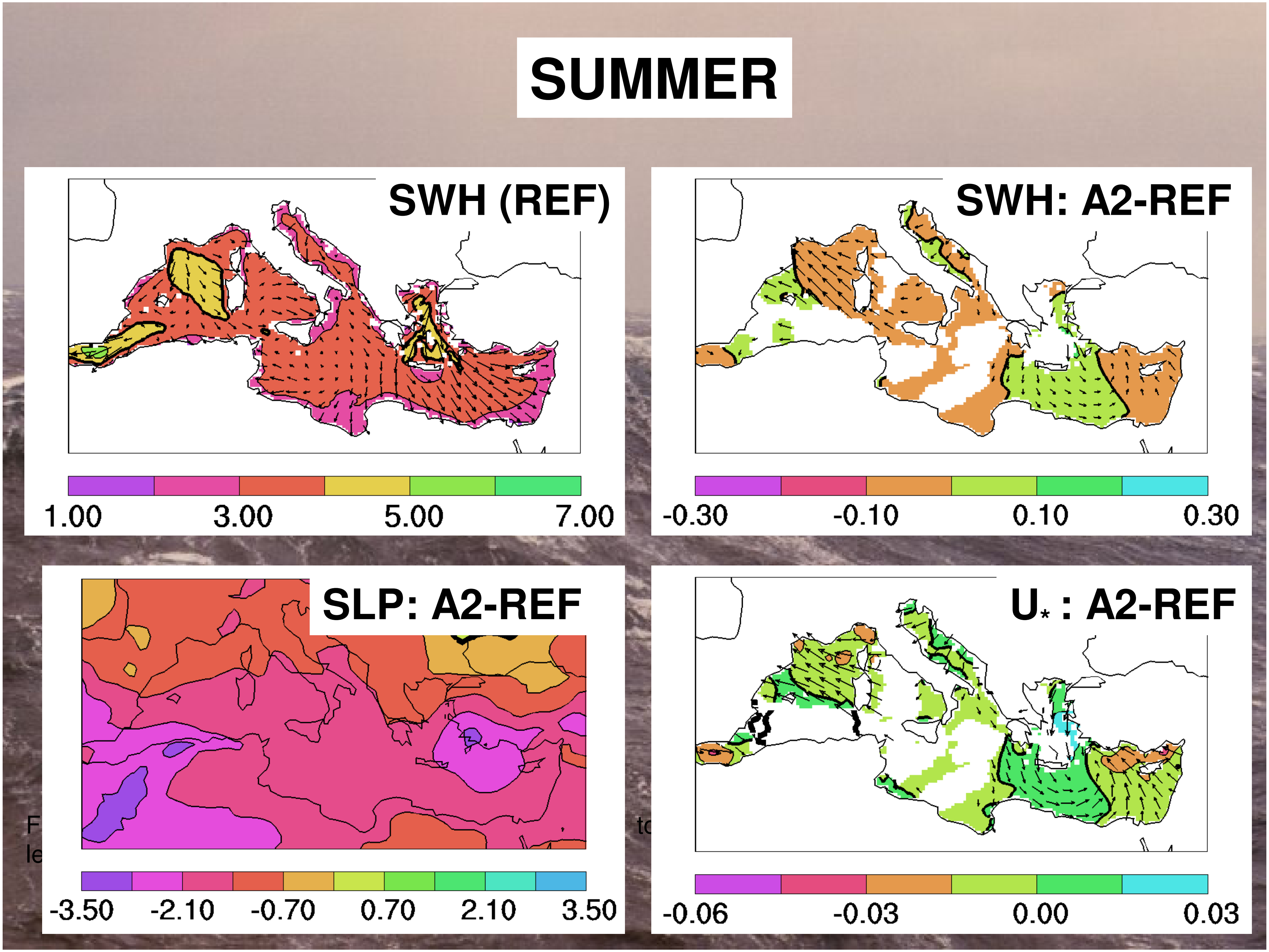
SUMMER
SWH (REF)
1.00 3.00 5.00 7.00
SWH: A2-REF
-0.30 -0.10 0.10 0.30
SLP: A2-REF
-3.50 -2.10 -0.70 0.70 2.10 3.50
U* : A2-REF
-0.06 -0.03 0.00 0.03

autumn

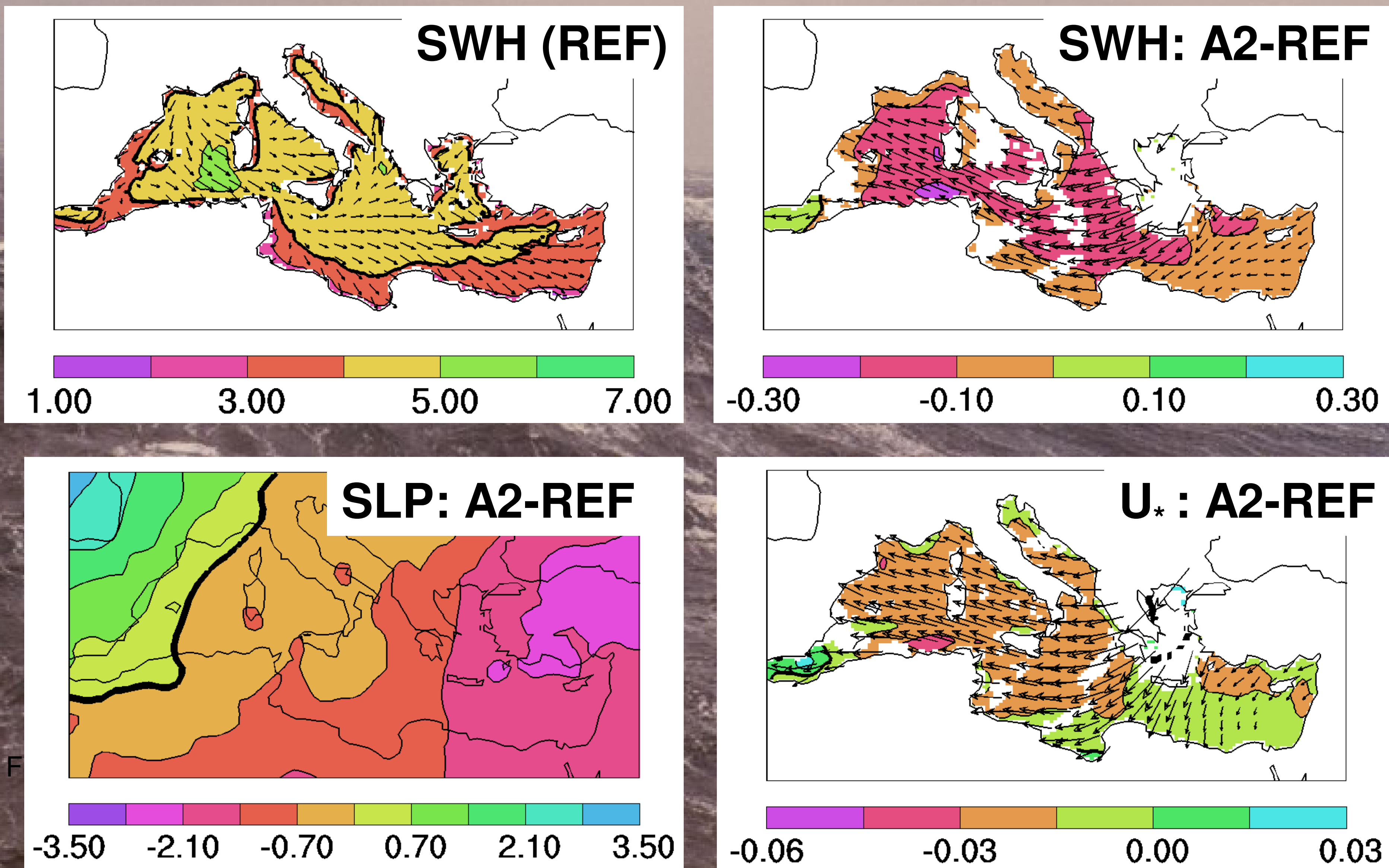
SWH (REF)
1.00 3.00 5.00 7.00
SWH: A2-REF
-0.30 -0.10 0.10 0.30
SLP: A2-REF
-3.50 -2.10 -0.70 0.70 2.10 3.50
F
U* : A2-REF
-0.06 -0.03 0.00 0.03

SWH: B2-REF

From Lionello et al 2008

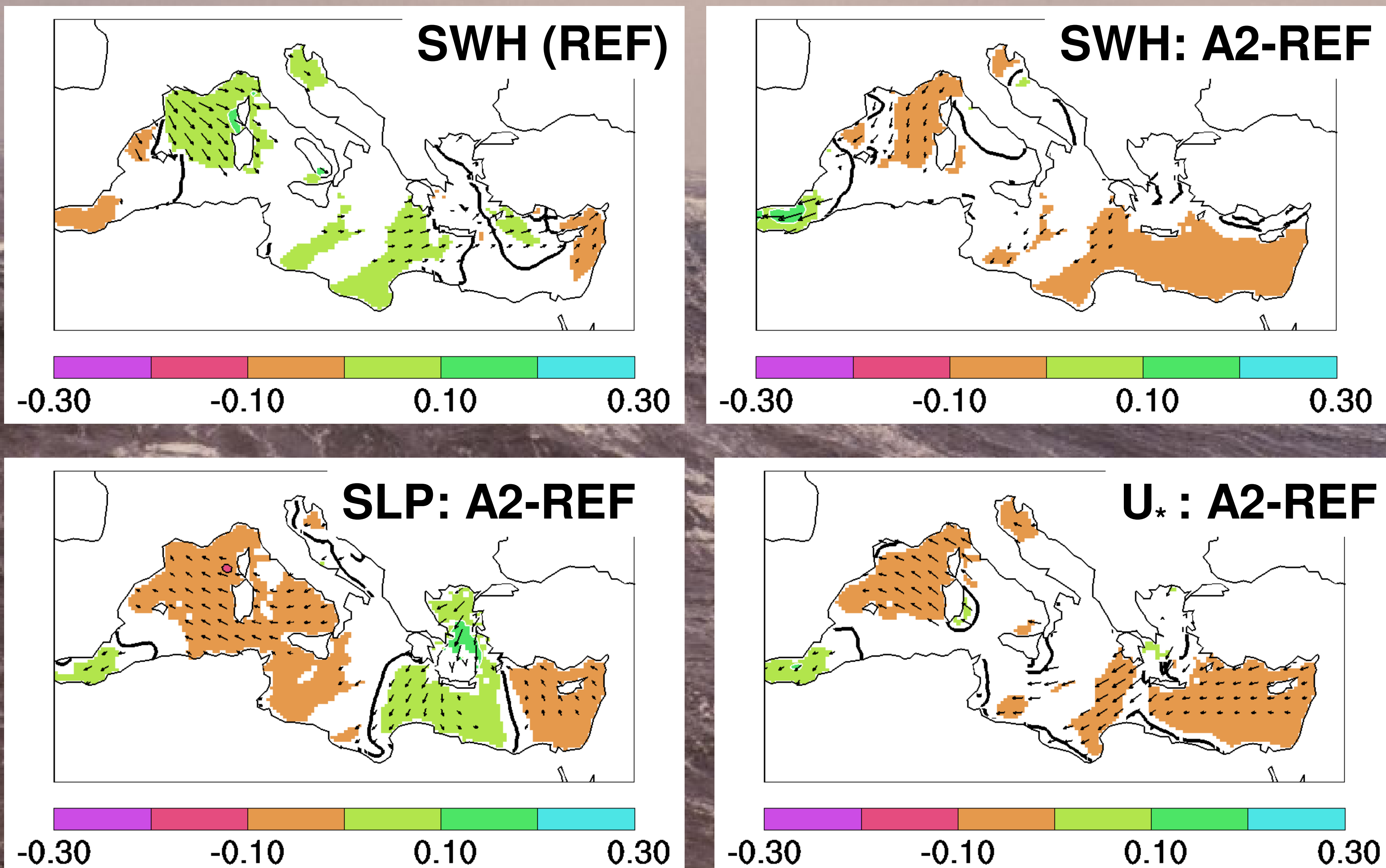

synthesis

During winter, in the second half of the 20th century, an overall decrease of cyclone activity has been observed in winter over the Mediterranean Sea. Generally this has produced lower mean SWH in winter and lower extremes

Regional interactions are complex and they cannot be explained by a single large scale TLC, so that several mid-latitude patterns are linked to the SWH field in the Mediterranean, especially for the cold season and the western part.

The decreasing mean SWH trend is projected to continue in future climate,

More simulations of future wave climate are needed to get an ensemble of simulations and to increase confidence on projections and assign a range of confidence to the results. High resolution simulations are needed to get a better dynamical basis for the estimate of the extremes.